

Carbamoyl Pyridone HIV-1 Integrase Inhibitors. 2. Bi- and Tricyclic Derivatives Result in Superior Antiviral and Pharmacokinetic Profiles

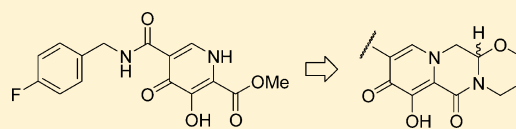
Takashi Kawasuji,^{*,†} Brian A. Johns,[‡] Hiroshi Yoshida,[†] Jason G. Weatherhead,[‡] Toshiyuki Akiyama,[†] Teruhiko Taishi,[†] Yoshiyuki Taoda,[†] Minako Mikamiyama-Iwata,[†] Hitoshi Murai,[†] Ryuichi Kiyama,[†] Masahiro Fujii,[†] Norihiko Tanimoto,[†] Tomokazu Yoshinaga,[†] Takahiro Seki,[†] Masanori Kobayashi,[†] Akihiko Sato,[†] Edward P. Garvey,[‡] and Tamio Fujiwara[†]

[†]Shionogi Pharmaceutical Research Center, Shionogi and Co., Ltd., 3-1-1, Futaba-cho, Toyonaka-shi, Osaka 561-0825, Japan

[‡]Infectious Diseases Therapeutic Area Unit, GlaxoSmithKline Research and Development, Five Moore Drive, Research Triangle Park, North Carolina 27709, United States

ABSTRACT: This work is a continuation of our initial discovery of a potent monocyclic carbamoyl pyridone human immunodeficiency virus type-1 (HIV-1) integrase inhibitor that displayed favorable antiviral and pharmacokinetic properties. We report herein a series of bicyclic carbamoyl pyridone analogues to address conformational issues from our initial SAR

studies. This modification of the core unit succeeded to deliver low nanomolar potency in standard antiviral assays. An additional hydroxyl substituent on the bicyclic scaffold provides remarkable improvement of antiviral efficacies against clinically relevant resistant viruses. These findings led to additional cyclic tethering of the naked hydroxyl group resulting in tricyclic carbamoyl pyridone inhibitors to address remaining issues and deliver potential clinical candidates. The tricyclic carbamoyl pyridone derivatives described herein served as the immediate leads in molecules to the next generation integrase inhibitor dolutegravir which is currently in late stage clinical evaluation.



1. INTRODUCTION

HIV-1 integrase (IN) is a virally encoded enzyme essential for replication that catalyzes the integration of viral DNA into the host chromatin. As a result of this unique retroviral step, IN has become an attractive target for drug discovery.¹ In 2007, raltegravir² (RAL) (Figure 1) became the first approved HIV-1 IN inhibitor (INI), thus opening up a new class of antiretroviral agents, and it has since become a preferred first line agent as part of the highly active antiretroviral therapy (HAART) treatment guidelines since 2009.³ RAL requires a 400 mg twice daily dose and has given rise to clear signature mutation pathways (N155H, Q148H/K/R-G140S, and Y143C).⁴ Elvitegravir⁵ (EVG) (Figure 1) is a second INI that was approved in 2012. EVG allows for a once daily dose of 150 mg; however, this requires coadministration of CYP3A inhibitor as a PK booster.⁶ Additionally, EVG has significant cross-resistance with RAL in both the N155 and Q148 mutation pathways.⁷ While both RAL and EVG are valued additions to the HAART armamentarium, there remains significant room for differentiation and improvement. It was our vision that a next generation INI would have to address attributes in the areas of overall dose burden, dosing interval,⁸ potency against resistant mutations and genetic barrier to resistance. Thus, it was with these goals that we set out to design a novel scaffold that would deliver clear value for patients. The work presented herein is the second in a series of manuscripts to elaborate on the evolution of our scaffold design in pursuit of true next generation properties that ultimately resulted in the discovery of dolutegravir (DTG) (Figure 1) to deliver low dose, once

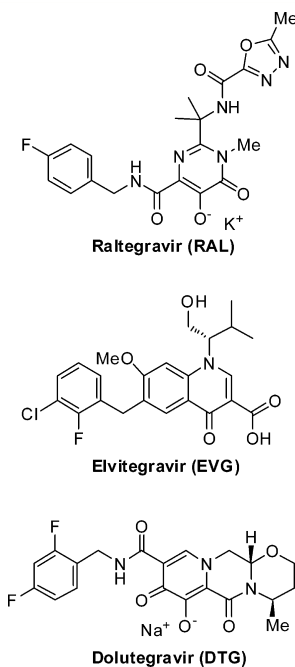


Figure 1. HIV-1 integrase inhibitors.

Received: October 23, 2012

Published: January 14, 2013

daily unboosted PK, and exceptional resistance properties.⁹ We recently reported on the two-metal pharmacophore¹⁰ driven design of a carbamoyl pyridone INI **1** shown in Figure 2a.¹¹

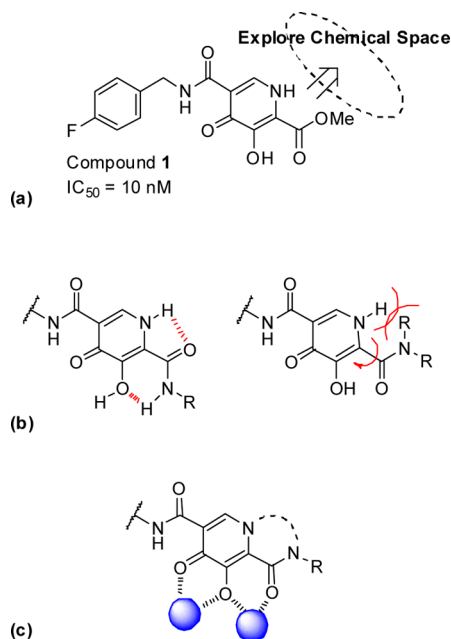


Figure 2. (a) Monocyclic carbamoyl pyridone lead inhibitor **1**. (b) Unfavorable intramolecular hydrogen bonding and steric hindrance potentially disrupt the coplanarity of the metal chelation motif by amide modifications. (c) Logical approach toward the cyclization modification to fix the metal chelation motif into a coplanar orientation.

This compound showed remarkable antiviral potency against wild-type HIV-1 virus from just the minimum pharmacophore elements consisting of C2 carboxylate and C3 hydroxy pyridone moiety as a basic chelating unit and a benzylcarboxamide unit to occupy the hydrophobic region. Although the potency against some clinically relevant mutant viruses was comparable to that of the prior generation INIs and insufficient for further development, this agent showed encouraging PK properties with a $T_{1/2}$ of 4.7 h and robust plasma drug levels well in excess of the protein adjusted IC_{50} ($^{MT4}PAIC_{50}$) at 24 h after oral dosing in rat PK studies. The initial monocyclic carbamoyl pyridone inhibitor **1** has an ester unit at the C2 position to coordinate with a metal cofactor in the catalytic active site of the enzyme. We sought to explore further chemical space adjacent to the requisite pharmacophore elements in hopes of addressing the potential risk of chemical or metabolic stabilities of the ester unit as well as attempting to improve on the remaining deficiencies around resistance profile. We initially tried amide derivatives including primary, secondary, and tertiary amides. Potentially the amide modification could provide an additional benefit in antiviral potency due to slightly higher basicity of carbonyl lone pair favorable to coordination with magnesium cofactors in the active site. However, potencies were remarkably reduced in both enzymatic and antiviral assays, presumably because the amide analogue causes an undesired intramolecular hydrogen bond between the central OH and amide NH moiety (in the case of primary and secondary amide examples) or more generally simply disrupts the coplanarity of the metal chelation motif due to steric hindrance of the amide and the pyridone

NH as shown in Figure 2b. Either way, this distortion of the chelating unit critical for effective binding to the adjoining two metal cofactors was not productive during the simple ester to amide modification. An intramolecular tethering design was adopted as shown in Figure 2c as a logical next step in the development of the carbamoyl pyridone SAR in order to fix the metal chelation motif into a desired coplanar orientation for effective metal coordination.

2. CHEMISTRY

All tested compounds were prepared through the key N1 acetaldehyde unit using one of the strategies outlined in Figure 3. Series A and B were accessed through imine formation which

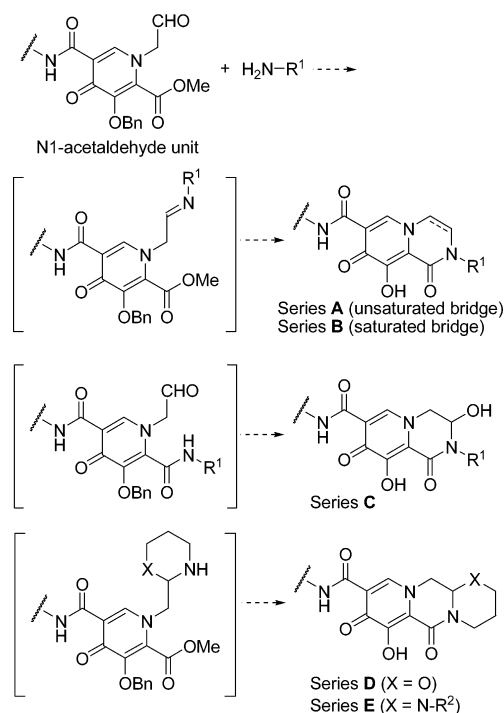
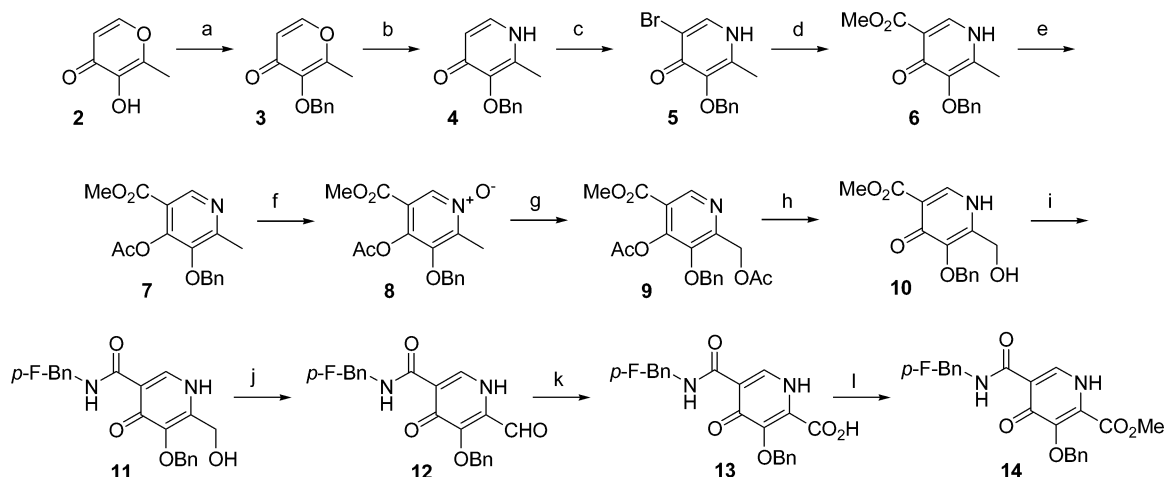


Figure 3. Conceptual synthetic approach toward bi- and tricyclic analogues.

underwent enamine tautomerization and led to the unsaturated analogues (series A) and upon reduction the saturated counterparts (series B). Condensation of the N1 acetaldehyde with a pendent amide led to the hydroxyl containing series C. Finally, access to the tricyclic series D or E was envisioned to result from condensation of the acetaldehyde functionalized core with an aminoalcohol or diamine which could then close to form a fused amide group and facilitate the tricyclic ring formation.

The key synthetic divergence points were chosen as the benzyl protected intermediates **13** and **14** (Scheme 1). These were chosen because of the potential for mild and selective modification of the core and C2 carboxyl moiety to support our synthetic strategies outlined in Figure 3. In addition, the benzyl protected central hydroxyl would be stably protected and able to be exposed chemoselectively in a last step to produce the fully functionalized metal binding moiety. The commercially available maltol **2** was protected as its benzyl ether followed by pyrone to pyridone conversion via amination with ammonia to provide intermediate **4**. C5 bromination was followed by palladium catalyzed carbonylation to give the methyl ester **6**.

Scheme 1. Synthesis of Key Intermediates^a

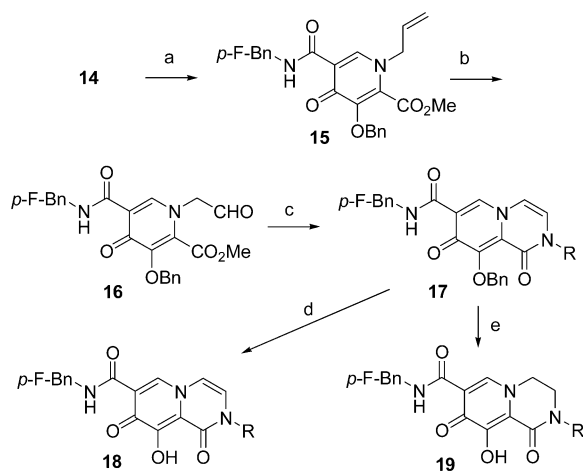
^aReagents and conditions: (a) BnBr, K₂CO₃, DMF, 80 °C; (b) NH₃, 2 M NaOH, ethanol, 90 °C; (c) *N*-bromosuccinimide, acetonitrile, rt; (d) Pd(OAc)₂, 1,3-bis(diphenylphosphino)propane, Et₃N, CO, methanol, DMF, 80 °C; (e) Ac₂O, 130 °C; (f) *m*-CPBA, chloroform, rt; (g) Ac₂O, 130 °C; (h) MeONa, methanol, rt; (i) 4-fluorobenzylamine, DMF, 120 °C; (j) MnO₂, chloroform, 60 °C; (k) NaCl, sulfamic acid, THF–water, rt; (l) HOBT, 1-ethyl-3-(3-dimethylaminopropyl)carbodiimide hydrochloride, Et₃N, methanol, DMF, reflux.

After acetyl protection of 4-hydroxyl, oxidation of the pyridine nitrogen with *m*-CPBA was performed followed by thermal rearrangement of the resultant *N*-oxide in acetic anhydride to give the corresponding C2-hydroxymethyl derivative **9**. The acetoxy unit was selectively removed with anhydrous sodium methoxide followed by amination with 4-fluorobenzylamine on the C5 ester to provide **11**. The C2 alcohol was oxidized in a stepwise manner to produce the corresponding carboxylic acid **13**. Condensation with methanol was performed to conclude preparation of intermediate **14**.

The synthesis of series A and B are shown in Scheme 2. *N*-Allylation of **14** and oxidative cleavage with osmium tetroxide

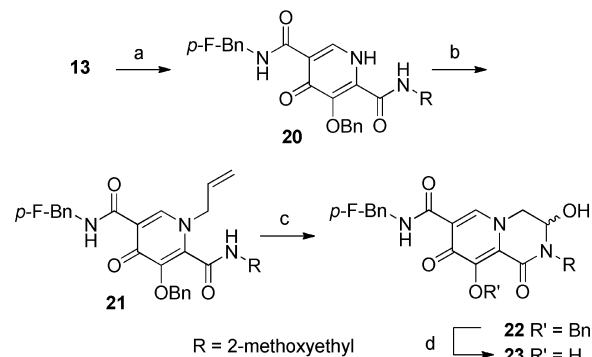
and sodium metaperiodate gave the corresponding acetaldehyde intermediate **16**. After formation of an imine with a primary amine, intramolecular cyclization proceeded using microwave heating to provide **17**. Acidic deprotection of **17** served to deprotect the above-mentioned benzyl ether and preserve the unsaturation to give the target series A derivatives **18a–f**. Subjecting **17** to hydrogenolysis conditions also resulted in removal of the benzyl ether while concomitantly reducing the newly formed ring to give the partially saturated compounds **19a–f** (series B).

Synthesis of series C is shown in Scheme 3. After amidation of the carboxylic acid **13** with a primary amine, *N*-allylation was

Scheme 2. Synthesis of Series A and B^a

[17–19]a : R = 2-methoxyethyl
 [17–19]b : R = 2-(*N*-morpholino)ethyl
 [17–19]c : R = 2-dimethylcarbamoylmethyl
 [17–19]d : R = 2-isopropoxyethyl
 [17–19]e : R = 2-phenoxyethyl
 [17–19]f : R = cyclohexyl

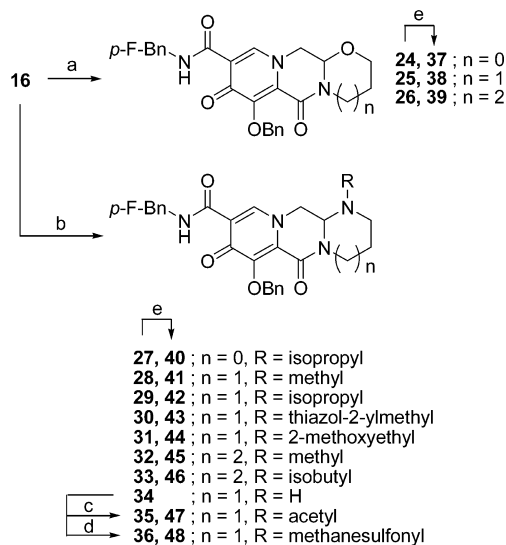
^aReagents and conditions: (a) 3-bromopropene, Cs₂CO₃, DMF, rt; (b) potassium osmate dihydrate, sodium metaperiodate, 1,4-dioxane, rt; (c) amine, dichloromethane, 140 °C microwave; (d) TFA, rt; (e) H₂, 10% Pd–C, DMF–methanol, rt.

Scheme 3. Synthesis of Series C^a

^aReagents and conditions: (a) HOBT, 1-ethyl-3-(3-dimethylaminopropyl)carbodiimide hydrochloride, Et₃N, DMF, reflux; (b) 3-bromopropene, Cs₂CO₃, DMF, rt; (c) potassium osmate dihydrate, sodium metaperiodate, 1,4-dioxane, rt; (d) 10% Pd–C, DMF–methanol, rt.

performed to give intermediate **21**. Oxidative cleavage of the double bond resulted in formation of hemiaminal derivatives **22**, and hydrogenolytic deprotection concluded the sequence to produce compound **23**.

Series D and E compounds were synthesized as shown in Scheme 4. The aldehyde **16** was condensed with an amino alcohol (series D) or diamine (series E) to generate the

Scheme 4. Synthesis of Series D and E^a

^aReagents and conditions: (a) amino alcohol, dichloromethane, 140 °C microwave; (b) diamine, dichloromethane, 140 °C microwave; (c) Ac₂O, cat. DMAP, pyridine, rt; (d) MsCl, DMAP, pyridine, rt; (e) 10% Pd–C, methanol, rt.

corresponding cyclic (hemi)aminal moiety and direct heating under microwave irradiation promoted intramolecular cyclization to provide the corresponding tricyclic compounds 24–36. Additional modification on the secondary amine of 34 allowed introduction of an acetyl or sulfonyl functional group.

Subsequent deprotection completed preparation of compounds 37–48.

3. RESULTS AND DISCUSSION

3.1. Antiviral Profiles of Bicyclic Series A and B.

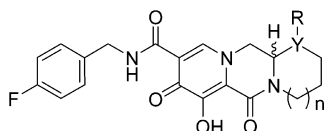
Inhibitory activities of series A and B are summarized in Table 1. Slightly improved antiviral potencies against wild type HIV-1 virus from the initial compound 1 were observed while the uniformly high selectivity index over cytotoxicity to indicate a true antiviral effect was maintained. Although variation on R did not have a significant influence on antiviral potency, modifications toward hydrophilic substituents appeared to have a negative impact on potency as seen in compounds 19b, 18c, and 19c. Potency shifts in presence of human serum albumin (HSA) resulted in a very acceptable protein adjustment to the IC₅₀ (^{MT4}PAIC₅₀). Comparison of series A (unsaturated) and series B (saturated) resulted in no significant difference in potency for the R groups that were examined; however, slightly larger protein shift was observed for the unsaturated analogues. The saturated series B also had a slightly improved profile (vs series A) against the Q148K site directed mutant virus across the R substituents examined. An improvement of fold change against the Q148K mutant compared to the original monocyclic compound 1 was observed in compounds that have an ethereal R group (18a, 19a, 18d, 19d, and 19e); however, the data still left room for improvement to achieve our original differentiation goals.

3.2. Antiviral Profiles of Hydroxyl Series C and Tricyclic Series D and E. A remarkable potency improvement against the Q148K variant was observed from hydroxyl compound 23 (IC₅₀ = 3.8 nM vs wild type with a 2.1-fold

Table 1. Antiviral Profiles of Series A and B^a

compd	R	MT-4/MTT ^b wild type IC ₅₀ (nM)	MT-4/MTT ^c CC ₅₀ (nM)	Q148K ^d (FC)	^{MT4} PAIC ₅₀ ^e (nM)	potency shift ^f
1	-	10 ± 2.9	19000 ± 850	200 ± 25	120	12
18a		1.6 ± 1.1	>200000	35 ± 6.8	27	17
19a		5.9 ± 0.044	52000 ± 8300	18 ± 2.5	18	3.1
18b		6.6 ± 1.5	36000 ± 4100	>250	20	3
19b		21 ± 5.5	160000 ± 25000	NT	34	1.6
18c		35 ± 8.8	>200000	NT	144	4.1
19c		26 ± 7.9	>200000	NT	62	2.4
18d		4.3 ± 1.4	49000 ± 19000	39 ± 14	19	4.4
19d		4.2 ± 1.0	30000 ± 1900	9.9 ± 1.3	13	3.1
18e		4.4 ± 1.6	2400 ± 710	>250	48	11
19e		6.8 ± 3.7	10000 ± 1300	17 ± 6.9	65	9.5
18f		12 ± 3.1	>200000	>250	156	13
19f		6.5 ± 2.9	>240000	>250	29	4.4

^aData represent the mean ± SD from three independent experiments. ^bAnti-HIV activities using MT-4 cells. ^cCytotoxicity using MT-4 cells. ^dFold change against the resistant variant. ^eProtein adjusted antiviral potencies based on MT-4/MTT IC₅₀. ^fPotency shift in presence of human serum albumin.

Table 2. Antiviral Profiles of Series C, D, and E^a


compd	Y	n	R	MT-4/MTT ^b wild type IC ₅₀ (nM)	MT-4/MTT ^c CC ₅₀ (nM)	Q148K ^d (FC)	MTT ^e PAIC ₅₀ ^e (nM)	potency shift ^f
23				3.8 ± 0.53	83000 ± 22000	2.1 ± 0.50	14.1	3.7
37	O	0		2.7 ± 0.63	72000 ± 24000	19 ± 5.1	140.4	52
38	O	1		3.4 ± 1.1	18000 ± 1600	2.8 ± 0.32	26.9	7.9
39	O	2		2.9 ± 0.70	26000 ± 7000	2.2 ± 1.2	22.0	7.6
40	N	0	isopropyl	2.3 ± 0.55	8000 ± 2500	39 ± 7.4	7.8	3.4
41	N	1	methyl	3.8 ± 0.96	20000 ± 3000	4.7 ± 1.0	16.3	4.3
42	N	1	isopropyl	7.5 ± 0.42	7200 ± 790	9.1 ± 1.7	32.3	4.3
43	N	1	thiazol-2-ylmethyl	3.3 ± 0.91	2800 ± 820	4.2 ± 1.6	12.9	3.9
44	N	1	2-methoxyethyl	5.2 ± 1.3	9800 ± 2200	5.7 ± 0.47	20.3	3.9
45	N	2	methyl	6.4 ± 3.7	>200000	4.2 ± 1.0	31.4	4.9
46	N	2	isobutyl	5.4 ± 0.92	13000 ± 5000	3.2 ± 1.1	91.8	17
47	N	1	acetyl	29 ± 4.2	>200000	NT	58.0	2
48	N	1	methanesulfonyl	43 ± 22	>220000	NT	120.4	2.8

^aData represent the mean ± SD from independent three experiments. ^bAnti-HIV activities using MT-4 cells. ^cCytotoxicity using MT-4 cells. ^dFold change against the resistant variant. ^eProtein adjusted antiviral potencies based on MT-4/MTT IC₅₀. ^fPotency shift in presence of human serum albumin.

Table 3. Resistance Profile against RAL Resistant Mutants and PK Parameters in Rat^a

compd	Q148K (FC)	N155H (FC)	Y143R (FC)	CLt (mL min ⁻¹ kg ⁻¹)	T _{1/2} (h)	Vd _{ss} (mL/kg)	F (%)	C ₂₄ /MT ⁴ PAIC ₅₀
RAL	83 ± 6.6 ^b	8.4 ± 1.8 ^b	16 ± 3.9 ^b					
EVG	>1700 ^b	25 ± 7.8 ^b	1.8 ± 0.16 ^b					
1	200 ± 25	21 ± 8.9	1.5 ± 0.59	1.2 ± 0.41	4.7 ± 0.15	200 ± 38	53 ± 20	3.4
18a	35 ± 6.8	3.7 ± 1.0	1.6 ± 0.40	0.02 ± 0.00	11 ± 2.6	15 ± 1.1	40 ± 7.1	2600
19a	18 ± 2.5	1.5 ± 0.16	1.5 ± 0.12	0.51 ± 0.04	3.4 ± 0.28	120 ± 6	41 ± 2.7	27
23	2.1 ± 0.50	1.5 ± 0.054	1.5 ± 0.28	0.24 ± 0.02	7.6 ± 0.2	140 ± 13	14 ± 6.3	117
38	2.8 ± 0.32	1.6 ± 0.75	1.6 ± 0.85	0.10 ± 0.03	17 ± 6.7	130 ± 11	51 ± 8.5	685

^aData represent the mean ± SD. FC: fold change. ^bData reported in ref 9.

reduction against Q148K). This potency profile combined with a very modest 3.7-fold shift in the presence of HSA served as encouragement for further exploration. However, as is discussed in the next section, the series C compound did not show sufficient oral bioavailability. Moreover, the hemiaminal chiral center is not configurationally stable and interconverts on a moderate time scale (minutes to hours), resulting in loss of enantiomeric purity after chiral purification. Additional series C derivatives wherein the R substituent was modified are not shown herein but delivered similar virological and PK profiles and hence were not further improvements to justify continued pursuit. Although we abandoned further exploration of series C, the hydroxyl substitution on the saturated bridge provided impetus to address the perceived PK and configurational stability issues. In order to address the immediate issue of configurational stability, two series of tricyclic analogues were devised whereby the hemiaminal was effectively "locked down" into a third ring such that equilibration through an open chain intermediate would not be feasible. The oxygen and nitrogen containing third ring analogues, series D and E, respectively, showed high antiviral potencies against wild-type virus and excellent selectivity over cytotoxicity as previously observed (Table 2). The ring size (five-, six-, and seven-member) does not affect antiviral efficacy for the wild type virus regardless of hemiaminal or aminated analogue; however, the five-membered analogues 37 and 40 lost potency against the mutant. Although the series E aminated unit does not appear to impact potency or

resistance profile significantly, hydrophilic functional groups as seen in 47 and 48 do begin to erode the antiviral activity.

3.3. Efficacy against Additional RAL Signature Pathways and Rat PK Profiles of 18a, 19a, 23, and 38. Antiviral potency against clinically relevant RAL resistant mutants (Q148K, N155H, and Y143R) and rat PK profiles are summarized in Table 3. The bicyclic analogues 18a, 19a, hydroxyl examples 23, and tricyclic analogue 38 showed a low fold change against the N155H and Y143R site directed against mutants. As was discussed above, the tricyclic derivatives furthermore succeeded in improving efficacy against Q148K which was the primary remaining issue left unaddressed by monocyclic lead analogue 1. Low dose rat PK profiles resulted in low CLt (1 mL min⁻¹ kg⁻¹) and moderate to long T_{1/2} estimates (3–17 h) in every compound in Table 3. Although the moderate to low oral bioavailability of the hydroxyl derivative 23 raised concerns, the tricyclic analogue 38 delivered a yet further improved T_{1/2} accompanied by an oral bioavailability of 50%. The rat 24 h plasma concentration (C₂₄) of 7127 ng/mL from a 5 mg/kg oral dose robustly covered the MT⁴PAIC₅₀ of 10 ng/mL. No remarkable CYP inhibition or metabolic concerns were identified during in vitro studies.

Although these virological advances and promising PK profile of the tricyclic series D were significant toward our goal, this data set was from racemate. As an initial approach to understand contributions of the individual enantiomers toward

the antiviral profile, the isomers were isolated after chiral chromatographic separation of the *O*-benzyl protected precursor **25** to give the enantiopure benzyl ethers **25R** and **25S**. Subsequent deprotection via hydrogenolysis provided the pure individual enantiomers **38R** and **38S** as shown in Figure 4.

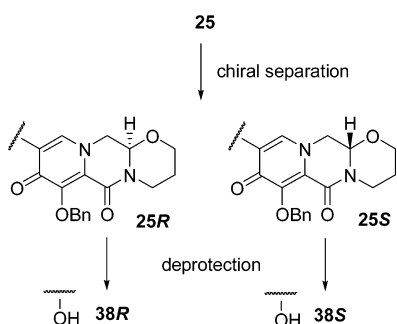


Figure 4. Chiral separation of compound **38**.

We were initially concerned that the hemiaminal stability would be an issue, but no interconversion or chemical stability issues were observed with the purified isomers of **38**. Notably the isomers had almost identical antiviral activity against wild type virus; however, they significantly differed in their loss of activity against a Q148K mutation. The *S* derivative displayed only a 2-fold potency change, while the *R* analogue had a 10-fold shift in potency. The isomers also showed different protein binding shifts with the *S* isomer showing a near 50-fold shift, while the *R* isomer had a very modest 5-fold loss of potency in the presence of HSA. These differences in protein binding on potency also suggest that a different PK profile might be expected to arise as well. These preliminary data on the purified isomers demonstrated excellent potency, and previous PK data from the racemate **38** were consistent with once daily PK potential with a low risk for CYP450 interaction and the need for a boosting agent.

5. CONCLUSIONS

The carbamoyl pyridone scaffold was optimized through a series of bicyclic and tricyclic analogues for the inhibition of HIV-1 IN utilizing a divergent synthetic strategy from a key *N*-pyridonyl-acetaldehyde intermediate. We have demonstrated that the addition of a second and third ring has added significant attributes to the carbamoyl pyridone core scaffold in terms of antiviral activity against both wild-type and key resistant mutants. Furthermore, protein binding effects as well as in vitro and in vivo PK profiles were taken into consideration in resulting in the optimization to the tricyclic analogues **38**. As such the tricyclic series D was identified as a true next generation INI series which appeared to deliver on our original differentiation goals centered on resistance and once daily PK. Further optimization of the individual enantiomers of compounds such as **38** will be the subject of future publications.

6. EXPERIMENTAL SECTION

6.1. Chemistry. Reactions were carried out under a nitrogen atmosphere with anhydrous solvents. Melting points were collected up to 300 °C with a Stanford Research Systems Optimelt for every crystallized sample. Purity of samples tested were assessed using combustion analyses or LC/MS/UV/ELSD, and the analytical data confirmed the purities to be $\geq 95\%$. Combustion analyses were performed with a Yanaco CORDER MT-6 and a DIONEX ICS-2000 instruments, and LC/MS/UV was performed with Waters Acquity

SQD system. Microwave irradiation was performed with Biotage Initiator. ^1H NMR spectra were measured on a Varian MERCURY or Gemini 300 MHz spectrometer in a solution of either CDCl_3 or $\text{DMSO}-d_6$, using tetramethylsilane as the internal standard. Chemical shifts are expressed as δ (ppm) values for protons relative to the internal standard.

3-Benzyloxy-2-methylpyran-4-one (3). Maltol **2** (189 g, 1.5 mol) was dissolved in DMF (1890 mL), and benzyl bromide (184 mL, 1.5 mol) was added. After the solution was stirred at 80 °C for 15 min, potassium carbonate (228 g, 1.65 mol) was added, and the mixture was stirred for 1 h. After the reaction solution was cooled to room temperature, the inorganic salt was filtered off, and the filtrate was evaporated in vacuo. To the precipitated inorganic salt was added THF (1000 mL), and the salt was filtered off. The filtrate was again evaporated in vacuo to obtain the product (329 g, quant) as a colorless solid. ^1H NMR (CDCl_3) δ 2.09 (s, 3H), 5.15 (s, 2H), 6.36 (d, $J = 5.6$ Hz, 1H), 7.29–7.41 (m, 5H), 7.60 (d, $J = 5.6$ Hz, 1H).

3-Benzyloxy-2-methyl-1H-pyridine-4-one (4). Compound **3** (162 g, 750 mmol) was dissolved in ethanol (487 mL), and aqueous ammonia (28%, 974 mL) and a 6 M aqueous sodium hydroxide solution (150 mL, 900 mmol) were added. After the reaction solution was stirred at 90 °C for 1 h, the solution was cooled under ice-cooling, and ammonium chloride (58 g, 1.08 mol) was added. The solution was extracted with chloroform, and the organic layer was washed with an aqueous saturated sodium bicarbonate solution and dried with anhydrous sodium sulfate. The solvent was evaporated in vacuo. Then isopropyl alcohol and diethyl ether were added to the residue. Precipitated solid was filtered to obtain the product (69.1 g, 43% yield) as a pale yellow solid. ^1H NMR ($\text{DMSO}-d_6$) δ 2.05 (s, 3H), 5.04 (s, 2H), 6.14 (d, $J = 7.2$ Hz, 1H), 7.31–7.42 (m, 5H), 7.46 (d, $J = 7.2$ Hz, 1H), 11.29 (brs, 1H).

3-Benzyloxy-5-bromo-2-methyl-1H-pyridine-4-one (5). Compound **4** (129 g, 599 mmol) was suspended in acetonitrile (1300 mL), and *N*-bromosuccinimide (117 g, 659 mmol) was added. After the mixture was stirred at room temperature for 1.5 h, precipitated crystals were filtered and washed with acetonitrile and diethyl ether to obtain the product (154 g, 88% yield) as a colorless solid. ^1H NMR ($\text{DMSO}-d_6$) δ 2.06 (s, 3H), 5.04 (s, 2H), 7.32–7.42 (m, 5H), 8.03 (d, $J = 5.5$ Hz, 1H), 11.82 (brs, 1H).

Methyl 5-Benzyloxy-6-methyl-4-oxo-1,4-dihydropyridine-3-carboxylate (6). To a solution of compound **5** (88.0 g, 300 mmol), $\text{Pd}(\text{OAc})_2$ (13.4 g, 60.0 mmol), and 1,3-bis(diphenylphosphino)propane (30.8 g, 516 mmol) in DMF (660 mL) were added methanol (264 mL) and triethylamine (210 mL, 1.50 mol) at room temperature. The interior of a reaction vessel was replaced with CO , and the solution was stirred at room temperature for 30 min, then stirred at 80 °C for 18 h. To a mixture of ethyl acetate (1500 mL), an aqueous saturated ammonium chloride solution (1500 mL), and water (1500 mL) stirred under ice-cooling was added the reaction solution. Precipitates were filtered and washed with water (300 mL), ethyl acetate (300 mL), and diethyl ether (300 mL) to obtain the product (44.9 g, 55% yield) as a colorless solid. ^1H NMR ($\text{DMSO}-d_6$) δ 2.06 (s, 3H), 3.72 (s, 3H), 5.02 (s, 2H), 7.33–7.42 (m, 5H), 8.07 (s, 1H).

Methyl 4-Acetoxy-5-benzyloxy-6-methylnicotinate (7). After a solution of compound **6** (19.1 g, 70.0 mmol) in acetic anhydride (134 mL) was stirred at 130 °C for 40 min, the acetic anhydride was evaporated in vacuo to obtain the product (19.9 g, 90% yield) as a flesh colored solid. ^1H NMR (CDCl_3) δ 2.29 (s, 3H), 2.52 (s, 3H), 3.89 (s, 3H), 4.98 (s, 2H), 7.36–7.41 (m, 5H), 8.85 (s, 1H).

Methyl 4-Acetoxy-5-benzyloxy-6-methyl-1-oxynicotinate (8). To a solution of compound **7** (46.2 g, 147 mmol) in chloroform (370 mL) was added 65% *m*-CPBA (42.8 g, 161 mmol) in portions under ice-cooling, and the solution was stirred at room temperature for 90 min. To the reaction solution was added a 10% aqueous potassium carbonate solution, and the mixture was stirred for 10 min. The solution was extracted with chloroform, and the organic layer was washed successively with a 10% aqueous potassium carbonate solution, an aqueous saturated ammonium chloride solution, and an aqueous saturated sodium chloride solution. The organic layer was dried with anhydrous sodium sulfate, and the solvent was evaporated in vacuo.

The residual precipitate was washed with diisopropyl ether to obtain the product (42.6 g, 87% yield) as a colorless solid. $^1\text{H NMR}$ (CDCl_3) δ 2.30 (s, 3H), 2.41 (s, 3H), 3.90 (s, 3H), 5.02 (s, 2H), 7.37–7.39 (m, 5H), 8.70 (s, 1H).

Methyl 4-Acetoxy-6-acetoxymethyl-5-benzyloxynicotinate (9). To acetic anhydride (500 mL) which had been heated at 130 °C was added compound 8 (42.6 g, 129 mmol) over 2 min, and the mixture was stirred for 20 min. The acetic anhydride was evaporated in vacuo to obtain the product (49.6 g, quant) as a black oil. $^1\text{H NMR}$ (CDCl_3) δ 2.10 (s, 3H), 2.28 (s, 3H), 3.91 (s, 3H), 5.07 (s, 2H), 5.20 (s, 2H), 7.35–7.41 (m, 5H), 8.94 (s, 1H).

Methyl 5-Benzyloxy-6-hydroxymethyl-4-oxo-1,4-dihydropyridine-3-carboxylate (10). To a solution of compound 9 (9.50 g, 25.4 mmol) in methanol (50 mL) was added a 28 wt % sodium methoxide methanol solution (7.35 mL, 38.1 mmol) under ice-cooling. The solution was stirred at room temperature for 30 min. To an ice-cooled saturated ammonium chloride aqueous solution was added the reaction solution, and the mixture was stirred for 30 min. Precipitated crystals were filtered and washed with water and diethyl ether to obtain the product (4.68 g, 64% yield) as a colorless solid. $^1\text{H NMR}$ ($\text{DMSO}-d_6$) δ 3.72 (s, 3H), 4.37 (s, 2H), 5.06 (s, 2H), 5.72 (s, 1H), 7.34–7.40 (m, 5H), 8.06 (s, 1H), 11.47 (brs, 1H).

5-Benzyloxy-N-(4-fluorobenzyl)-6-hydroxymethyl-4-oxo-1,4-dihydropyridine-3-carboxamide (11). To a solution of compound 10 (289 mg, 1.0 mmol) in DMF (3 mL) was added 4-fluorobenzylamine (126 μL , 1.10 mmol). The mixture was stirred at 120 °C for 1.5 h. After the reaction solution was cooled to room temperature, 2 M aqueous HCl (6 mL) was added. The solution was extracted with ethyl acetate, and the organic layer was washed with water and an aqueous saturated sodium chloride solution. The organic layer was dried with anhydrous sodium sulfate, and the solvent was evaporated in vacuo to obtain the product (198 mg, 52% yield) as a colorless solid. $^1\text{H NMR}$ ($\text{DMSO}-d_6$) δ 4.45 (d, $J = 5.0$ Hz, 2H), 4.52 (d, $J = 6.0$ Hz, 2H), 5.09 (s, 2H), 5.84 (t, $J = 5.0$ Hz, 1H), 7.14–7.20 (m, 2H), 7.35–7.40 (m, 7H), 8.30 (s, 1H), 10.72 (t, $J = 6.0$ Hz, 1H), 11.97 (s, 1H).

5-Benzyloxy-N-(4-fluorobenzyl)-6-formyl-4-oxo-1,4-dihydropyridine-3-carboxamide (12). To a suspension of compound 11 (9.80 g, 25.6 mmol) in chloroform (490 mL) was added manganese dioxide (49.0 g). The mixture was stirred at room temperature for 1 h, then stirred at 60 °C for 20 min. The manganese dioxide was filtrated off under Celite filtration and washed with chloroform heated at 50 °C. The filtrate was evaporated in vacuo to obtain the product (8.20 g, 84% yield) as a pale yellow solid. $^1\text{H NMR}$ ($\text{DMSO}-d_6$) δ 4.53 (d, $J = 5.8$ Hz, 2H), 5.38 (s, 2H), 7.15–7.21 (m, 2H), 7.35–7.46 (m, 7H), 8.33 (s, 1H), 9.90 (s, 1H), 10.35 (t, $J = 5.8$ Hz, 1H), 12.49 (s, 1H).

3-Benzyloxy-5-(4-fluorobenzylcarbamoyl)-4-oxo-1,4-dihydropyridine-2-carboxylic Acid (13). To an aqueous solution (105 mL) of sodium chlorite (7.13 g, 78.8 mmol) and sulfamic acid (7.65 g, 78.8 mmol) was added a solution of compound 12 (15.0 g, 39.4 mmol) in THF (630 mL) under ice-cooling. The mixture was stirred at room temperature for 1 h, and water (2500 L) was added to the reaction solution. The precipitated crystals were filtered and washed with diethyl ether to obtain the product (14.0 g, 90% yield) as a colorless solid. $^1\text{H NMR}$ ($\text{DMSO}-d_6$) δ 4.52 (d, $J = 5.8$ Hz, 2H), 5.13 (s, 2H), 7.14–7.19 (m, 2H), 7.31–7.40 (m, 5H), 7.47–7.49 (m, 2H), 8.31 (d, $J = 4.5$ Hz, 1H), 10.44 (t, $J = 5.8$ Hz, 1H), 12.47 (brs, 1H).

Methyl 3-Benzyloxy-5-(4-fluorobenzylcarbamoyl)-4-oxo-1,4-dihydropyridine-2-carboxylate (14). Compound 13 (12.0 g, 30.3 mmol), 1-(3-dimethylaminopropyl)-3-ethylcarbodiimide hydrochloride (6.96 g, 36.3 mmol), and 1-hydroxybenzotriazole (4.91 g, 36.3 mmol) in DMF (180 mL) was stirred at room temperature for 1.5 h. To the mixture methanol (180 mL) and triethylamine (9.29 mL, 66.7 mmol) were added, and the mixture was heated to reflux for 1.5 h. The reaction solution was diluted with ethyl acetate, then washed with an aqueous saturated sodium bicarbonate solution, a 10% aqueous citric acid solution, and an aqueous saturated sodium chloride solution. The organic layer was dried with anhydrous sodium sulfate, and the solvent was evaporated in vacuo. The residual precipitate was washed with

diethyl ether to obtain the product (8.74 g, 70% yield) as a colorless crystals. $^1\text{H NMR}$ ($\text{DMSO}-d_6$) δ 3.85 (s, 3H), 4.52 (d, $J = 6.0$ Hz, 2H), 5.15 (s, 2H), 7.13–7.21 (m, 2H), 7.31–7.47 (m, 7H), 8.33 (s, 1H), 10.41 (t, $J = 6.0$ Hz, 1H), 12.59 (s, 1H).

Methyl 1-Allyl-3-benzyloxy-5-(4-fluorobenzylcarbamoyl)-4-oxo-1,4-dihydropyridine-2-carboxylate (15). To a solution of compound 14 (6.79 g, 16.5 mmol) were added 3-bromopropene (2.15 mL, 24.8 mmol) and Cs_2CO_3 (8.09 g, 24.8 mmol) in DMF (54 mL), and the mixture was stirred at room temperature for 4.5 h. To the reaction solution was added an aqueous ammonium chloride solution, and the mixture was extracted with ethyl acetate. The organic layer was washed with water and an aqueous saturated sodium chloride solution. The organic layer was dried with anhydrous sodium sulfate, and the solvent was evaporated in vacuo. The residual precipitate was washed with diethyl ether to obtain the product (6.15 g, 83% yield) as a colorless solid. $^1\text{H NMR}$ (CDCl_3) δ 3.76 (s, 3H), 4.54 (d, $J = 6.0$ Hz, 2H), 4.60 (d, $J = 6.0$ Hz, 2H), 5.20–5.37 (m, 2H), 5.25 (s, 2H), 5.80–5.93 (m, 1H), 6.98–7.04 (m, 2H), 7.31–7.35 (m, 7H), 8.45 (s, 1H), 10.41 (m, 1H).

Methyl 3-Benzyloxy-5-(4-fluorobenzylcarbamoyl)-4-oxo-1-(2-oxoethyl)-1,4-dihydropyridine-2-carboxylate (16). To a solution of compound 15 (7.6 g, 16.9 mmol) in 1,4-dioxane (228 mL) was added an aqueous solution (38 mL) of potassium osmate dihydrate (372 mg, 1.01 mmol), and sodium metaperiodate (14.5 g, 67.6 mmol) was further added. After being stirred at room temperature for 2 h the reaction solution was added to a vessel to which ethyl acetate (300 mL) and water (300 mL) had been added, while stirring. The organic layer was washed with water, a 5% aqueous sodium hydrogen sulfite solution and an aqueous saturated sodium chloride solution. The organic layer was dried with anhydrous sodium sulfate, and the solvent was evaporated in vacuo. The residual precipitate was washed with diethyl ether to obtain the product (5.39 g, 71% yield) as a colorless solid. $^1\text{H NMR}$ (CDCl_3) δ 3.74 (s, 3H), 4.60 (d, $J = 5.9$ Hz, 2H), 4.87 (s, 2H), 5.27 (s, 2H), 6.98–7.04 (m, 2H), 7.30–7.40 (m, 7H), 8.39 (s, 1H), 9.58 (s, 1H), 10.38 (s, 1H).

9-Benzyloxy-2-(2-methoxyethyl)-1,8-dioxo-1,8-dihydro-2H-pyrido[1,2-*a*]pyrazine-7-carboxylic Acid 4-Fluorobenzylamide (17a). To a solution of compound 16 (400 mg, 0.884 mmol) in dichloromethane (12 mL) were added 2-methoxyethylamine (77.0 μL , 0.884 mmol) and acetic acid (18 μL). After the mixture was stirred at room temperature for 5 min, the reaction was performed at 140 °C for 30 min in a microwave reaction apparatus. The solvent was evaporated in vacuo, and the residue was subjected to silica gel column chromatography. Fractions eluting with toluene–acetone were collected and evaporated in vacuo to obtain the product (226 mg, 54% yield) as a yellow solid. $^1\text{H NMR}$ (CDCl_3) δ 3.35 (s, 3H), 3.65 (t, $J = 5.2$ Hz, 2H), 3.98 (t, $J = 5.2$ Hz, 2H), 4.62 (d, $J = 6.0$ Hz, 2H), 5.28 (s, 2H), 6.57 (s, 2H), 6.98–7.04 (m, 2H), 7.30–7.38 (m, 5H), 7.637.67 (m, 2H), 8.59 (s, 1H), 10.60–10.64 (m, 1H).

9-Benzyloxy-2-[2-(morpholin-4-yl)ethyl]-1,8-dioxo-1,8-dihydro-2H-pyrido[1,2-*a*]pyrazine-7-carboxylic Acid 4-Fluorobenzylamide (17b). $^1\text{H NMR}$ (CDCl_3) δ 2.59 (s, 4H), 2.74 (s, 2H), 3.73 (s, 4H), 3.95 (s, 2H), 4.62 (d, $J = 6.0$ Hz, 2H), 5.28 (s, 2H), 6.53 (d, $J = 6.0$ Hz, 1H), 6.63 (d, $J = 6.0$ Hz, 1H), 7.01 (t, $J = 8.7$ Hz, 2H), 7.26–7.38 (m, 5H), 7.64 (d, $J = 6.9$ Hz, 2H), 8.61 (s, 1H), 10.61 (t, $J = 5.4$ Hz, 1H).

9-Benzyloxy-2-dimethylcarbamoylmethyl-1,8-dioxo-1,8-dihydro-2H-pyrido[1,2-*a*]pyrazine-7-carboxylic Acid 4-Fluorobenzylamide (17c). $^1\text{H NMR}$ (CDCl_3) δ 3.01 (s, 3H), 3.13 (s, 3H), 4.59 (s, 2H), 4.63 (d, $J = 6.0$ Hz, 2H), 5.26 (s, 2H), 6.42 (d, $J = 6.0$ Hz, 1H), 6.64 (d, $J = 6.0$ Hz, 1H), 6.98–7.05 (m, 2H), 7.16–7.36 (m, 5H), 7.60–7.66 (m, 2H), 8.60 (s, 1H), 10.59 (brt, $J = 6.0$ Hz, 1H).

9-Benzyloxy-2-(2-isopropoxyethyl)-1,8-dioxo-1,8-dihydro-2H-pyrido[1,2-*a*]pyrazine-7-carboxylic Acid 4-Fluorobenzylamide (17d). $^1\text{H NMR}$ (CDCl_3) δ 1.12 (d, $J = 6.0$ Hz, 6H), 3.51–3.59 (m, 1H), 3.68 (t, $J = 4.8$ Hz, 2H), 3.96 (t, $J = 4.8$ Hz, 2H), 4.62 (d, $J = 6.0$ Hz, 2H), 5.28 (s, 2H), 6.58–6.64 (m, 2H), 6.98–7.04 (m, 2H), 7.30–7.39 (m, 5H), 7.64–7.66 (m, 2H), 8.59 (brs, 1H), 10.63 (s, 1H).

9-Benzyloxy-1,8-dioxo-2-(2-phenoxyethyl)-1,8-dihydro-2H-pyrido[1,2-*a*]pyrazine-7-carboxylic Acid 4-Fluorobenzylamide (17e). $^1\text{H NMR}$ (CDCl_3) δ 4.17–4.20 (m, 2H), 4.25–4.28 (m, 2H),

4.62 (d, $J = 5.6$ Hz, 2H), 5.28 (s, 2H), 6.60–6.66 (m, 2H), 6.86 (d, $J = 8.0$ Hz, 2H), 6.95–7.04 (m, 2H), 7.28–7.37 (m, 8H), 7.64 (d, $J = 7.0$ Hz, 2H), 8.59 (s, 1H), 10.60 (brs, 1H).

9-Benzyloxy-2-cyclohexyl-1,8-dioxo-1,8-dihydro-2H-pyrido[1,2-*a*]pyrazine-7-carboxylic Acid 4-Fluorobenzylamide (17f). ^1H NMR (CDCl_3) δ 1.15–1.92 (m, 10H), 4.62 (d, $J = 6.1$ Hz, 2H), 4.70–4.78 (m, 1H), 5.27 (s, 2H), 6.43 (d, $J = 6.4$ Hz, 1H), 6.69 (d, $J = 6.3$ Hz, 1H), 7.01–7.16 (m, 2H), 7.18–7.37 (m, 5H), 7.66–7.68 (m, 2H), 8.63 (s, 1H), 10.67 (t, $J = 5.5$ Hz, 1H).

9-Hydroxy-2-(2-methoxyethyl)-1,8-dioxo-1,8-dihydro-2H-pyrido[1,2-*a*]pyrazine-7-carboxylic Acid 4-Fluorobenzylamide (18a). To compound 17a (140 mg, 0.293 mmol) was added trifluoroacetic acid (1.4 mL) under ice-cooling. The mixture was stirred at 0 °C for 5 min and at room temperature for 1.5 h. The solvent was evaporated in vacuo, and the residue was diluted with chloroform and ice-water. The organic layer was washed with an aqueous saturated sodium bicarbonate solution, a 10% aqueous citric acid solution and water. The organic layer was dried with anhydrous sodium sulfate, and the solvent was evaporated in vacuo. The residual crystals were recrystallized with dichloromethane-ethanol to obtain the product (89.0 mg, 79% yield) as yellow crystals. Mp 223–224 °C; ^1H NMR ($\text{DMSO-}d_6$) δ 3.25 (s, 3H), 3.58 (t, $J = 5.4$ Hz, 2H), 3.92 (t, $J = 5.1$ Hz, 2H), 4.53 (d, $J = 5.7$ Hz, 2H), 6.87 (d, $J = 6.3$ Hz, 1H), 7.14 (t, $J = 9.0$ Hz, 2H), 7.33–7.38 (m, 2H), 7.47 (d, $J = 6.0$ Hz, 1H), 8.77 (s, 1H), 10.56 (t, $J = 6.0$ Hz, 1H), 12.00 (brs, 1H). Anal. Calcd for $\text{C}_{19}\text{H}_{18}\text{FN}_3\text{O}_5$: C, 58.91; H, 4.68; F, 4.90; N, 10.85. Found: C, 58.68; H, 4.63; F, 4.73; N, 10.80.

9-Hydroxy-2-[2-(morpholin-4-yl)ethyl]-1,8-dioxo-1,8-dihydro-2H-pyrido[1,2-*a*]pyrazine-7-carboxylic Acid 4-Fluorobenzylamide (18b). Mp 212–215 °C; ^1H NMR ($\text{DMSO-}d_6$) δ 2.51 (s, 4H), 2.38 (s, 2H), 3.55 (s, 4H), 3.90 (s, 2H), 4.55 (d, $J = 6.0$ Hz, 2H), 6.95 (d, $J = 6.3$ Hz, 2H), 7.17 (t, $J = 8.7$ Hz, 2H), 7.35–7.40 (m, 2H), 7.50 (d, $J = 6.3$ Hz, 1H), 8.78 (s, 1H), 10.58 (t, $J = 6.3$ Hz, 1H), 12.10 (s, 1H). LC/MS: m/z 443 $[\text{M} + \text{H}]^+$.

2-Dimethylcarbamoylmethyl-9-hydroxy-1,8-dioxo-1,8-dihydro-2H-pyrido[1,2-*a*]pyrazine-7-carboxylic Acid 4-Fluorobenzylamide (18c). Mp >300 °C; ^1H NMR ($\text{DMSO-}d_6$) δ 2.87 (s, 3H), 3.03 (s, 3H), 4.55 (d, $J = 6.0$ Hz, 2H), 4.71 (s, 2H), 6.80 (d, $J = 6.3$ Hz, 1H), 7.16 (m, 2H), 7.38 (m, 2H), 7.48 (d, $J = 6.3$ Hz, 1H), 8.82 (s, 1H), 10.54 (brt, $J = 6.0$ Hz, 1H), 11.83 (s, 1H). Anal. Calcd for $\text{C}_{20}\text{H}_{19}\text{FN}_4\text{O}_5(\text{H}_2\text{O})_{0.4}$: C, 56.98; H, 4.73; F, 4.51; N, 13.29. Found: C, 57.03; H, 4.44; F, 4.50; N, 13.13.

9-Hydroxy-2-(2-isopropoxyethyl)-1,8-dioxo-1,8-dihydro-2H-pyrido[1,2-*a*]pyrazine-7-carboxylic Acid 4-Fluorobenzylamide (18d). Mp 209–210 °C; ^1H NMR ($\text{DMSO-}d_6$) δ 1.06 (d, $J = 6.3$ Hz, 6H), 3.54–3.64 (m, 3H), 3.90 (t, $J = 5.4$ Hz, 2H), 4.62 (d, $J = 6.0$ Hz, 2H), 6.89 (d, $J = 6.3$ Hz, 1H), 7.13–7.19 (m, 2H), 7.35–7.39 (m, 2H), 7.47 (d, $J = 6.3$ Hz, 1H), 8.77 (s, 1H), 10.58 (t, $J = 5.7$ Hz, 1H), 12.04 (brs, 1H). Anal. Calcd for $\text{C}_{21}\text{H}_{22}\text{FN}_3\text{O}_5$: C, 60.72; H, 5.34; F, 4.57; N, 10.12. Found: C, 60.78; H, 5.29; F, 4.34; N, 10.11.

9-Hydroxy-1,8-dioxo-2-(2-phenoxylethyl)-1,8-dihydro-2H-pyrido[1,2-*a*]pyrazine-7-carboxylic Acid 4-Fluorobenzylamide (18e). Mp 237–239 °C; ^1H NMR (CDCl_3) δ 4.18–4.21 (m, 2H), 4.26–4.29 (m, 2H), 4.62 (d, $J = 5.7$ Hz, 2H), 6.57 (d, $J = 6.3$ Hz, 1H), 6.71 (d, $J = 6.3$ Hz, 1H), 6.86 (d, $J = 8.1$ Hz, 2H), 6.97–7.02 (m, 3H), 7.29–7.35 (m, 4H), 8.56 (s, 1H), 10.58 (t, $J = 5.7$ Hz, 1H), 11.84 (brs, 1H). Anal. Calcd for $\text{C}_{24}\text{H}_{20}\text{FN}_3\text{O}_5$: C, 64.14; H, 4.49; F, 4.23; N, 9.35. Found: C, 64.46; H, 4.50; F, 4.01; N, 9.12.

2-Cyclohexyl-9-hydroxy-1,8-dioxo-1,8-dihydro-2H-pyrido[1,2-*a*]pyrazine-7-carboxylic Acid 4-Fluorobenzylamide (18f). Mp >300 °C; ^1H NMR ($\text{DMSO-}d_6$) δ 1.15–1.84 (m, 10H), 4.43–4.49 (m, 1H), 4.53 (d, $J = 5.8$ Hz, 2H), 7.05 (d, $J = 6.4$ Hz, 1H), 7.13–7.19 (m, 2H), 7.34–7.39 (m, 2H), 7.53 (d, $J = 6.4$ Hz, 1H), 8.79 (s, 1H), 10.61 (t, $J = 5.8$ Hz, 1H), 12.23 (brs, 1H). LC/MS: m/z 412 $[\text{M} + \text{H}]^+$.

9-Hydroxy-2-(2-methoxyethyl)-1,8-dioxo-1,3,4,8-tetrahydro-2H-pyrido[1,2-*a*]pyrazine-7-carboxylic Acid 4-Fluorobenzylamide (19a). Compound 17a (157 mg, 0.329 mmol) was dissolved in DMF (18 mL) and methanol (1 mL), and 10% palladium-carbon powder (31 mg) was added. The mixture was stirred at room temperature for 20 h under hydrogen atmosphere. The

reaction solution was filtered with Celite, and the filtrate was evaporated in vacuo. The residue was dissolved in chloroform, and insoluble residue was filtered with Celite again. The filtrate was evaporated in vacuo. The residual crystals were recrystallized from dichloromethane-methanol to obtain the product (66 mg, 52% yield) as brown crystals. Mp 197–199 °C; ^1H NMR ($\text{DMSO-}d_6$) δ 3.27 (s, 3H), 3.55 (t, $J = 5.1$ Hz, 2H), 3.68 (t, $J = 5.1$ Hz, 2H), 3.79 (s, 2H), 4.36 (s, 2H), 4.51 (d, $J = 5.7$ Hz, 2H), 7.15 (t, $J = 8.7$ Hz, 2H), 7.32–7.37 (m, 2H), 8.38 (s, 1H), 10.46 (t, $J = 5.4$ Hz, 1H), 12.41 (s, 1H). LC/MS: m/z 390 $[\text{M} + \text{H}]^+$.

9-Hydroxy-2-[2-(morpholin-4-yl)ethyl]-1,8-dioxo-1,3,4,8-tetrahydro-2H-pyrido[1,2-*a*]pyrazine-7-carboxylic Acid 4-Fluorobenzylamide (19b). Mp 205–207 °C; ^1H NMR ($\text{DMSO-}d_6$) δ 2.43 (s, 2H), 2.50 (s, 4H), 3.54 (s, 4H), 3.63 (s, 2H), 3.81 (s, 2H), 4.40 (s, 2H), 4.52 (d, $J = 6.0$ Hz, 2H), 7.16 (t, $J = 9.0$ Hz, 2H), 7.33–7.37 (m, 2H), 8.43 (s, 1H), 10.45 (t, $J = 5.7$ Hz, 1H), 12.48 (s, 1H). LC/MS: m/z 445 $[\text{M} + \text{H}]^+$.

2-Dimethylcarbamoylmethyl-9-hydroxy-1,8-dioxo-1,3,4,8-tetrahydro-2H-pyrido[1,2-*a*]pyrazine-7-carboxylic Acid 4-Fluorobenzylamide (19c). Mp 245 °C; ^1H NMR (CDCl_3) δ 3.00 (s, 3H), 3.08 (s, 3H), 3.83–3.87 (m, 2H), 4.37–4.41 (m, 2H), 4.42 (s, 2H), 4.60 (s, 2H), 6.98–7.04 (m, 2H), 7.30–7.34 (m, 2H), 8.33 (s, 1H). LC/MS: m/z 417 $[\text{M} + \text{H}]^+$.

9-Hydroxy-2-(2-isopropoxyethyl)-1,8-dioxo-1,3,4,8-tetrahydro-2H-pyrido[1,2-*a*]pyrazine-7-carboxylic Acid 4-Fluorobenzylamide (19d). Mp 210–212 °C; ^1H NMR ($\text{DMSO-}d_6$) δ 1.08 (d, $J = 6.0$ Hz, 6H), 3.54–3.66 (m, 5H), 3.79–3.83 (m, 2H), 4.35–4.39 (m, 2H), 4.52 (d, $J = 6.0$ Hz, 2H), 7.12–7.18 (m, 2H), 7.32–7.37 (m, 2H), 8.40 (s, 1H), 10.44 (t, $J = 6.0$ Hz, 1H), 12.42 (brs, 1H). Anal. Calcd for $\text{C}_{21}\text{H}_{24}\text{FN}_3\text{O}_5(\text{H}_2\text{O})_{0.3}$: C, 59.65; H, 5.86; F, 4.49; N, 9.94. Found: C, 59.58; H, 5.63; F, 4.40; N, 9.96.

9-Hydroxy-1,8-dioxo-2-(2-phenoxylethyl)-1,3,4,8-tetrahydro-2H-pyrido[1,2-*a*]pyrazine-7-carboxylic Acid 4-Fluorobenzylamide (19e). Mp 200–201 °C; ^1H NMR (CDCl_3) δ 3.96–4.02 (m, 4H), 4.20–4.28 (m, 4H), 4.60 (d, $J = 6.0$ Hz, 2H), 6.86–6.89 (m, 2H), 6.96–7.02 (m, 3H), 7.28–7.34 (m, 4H), 8.31 (s, 1H), 10.43 (brs, 1H), 12.15 (brs, 1H). Anal. Calcd for $\text{C}_{24}\text{H}_{20}\text{FN}_3\text{O}_5$: C, 63.85; H, 4.91; F, 4.21; N, 9.31. Found: C, 63.72; H, 4.93; F, 4.07; N, 9.29.

2-Cyclohexyl-9-hydroxy-1,8-dioxo-1,3,4,8-tetrahydro-2H-pyrido[1,2-*a*]pyrazine-7-carboxylic Acid 4-Fluorobenzylamide (19f). Mp >300 °C; ^1H NMR ($\text{DMSO-}d_6$) δ 1.03–1.81 (m, 10H), 3.69–3.72 (m, 2H), 4.29–4.36 (m, 3H), 4.52 (d, $J = 6.1$ Hz, 2H), 7.13–7.19 (m, 2H), 7.33–7.37 (m, 2H), 8.43 (s, 1H), 10.47 (t, $J = 5.8$ Hz, 1H), 12.59 (brs, 1H). LC/MS: m/z 414 $[\text{M} + \text{H}]^+$.

3-Benzyloxy-*N*⁵-(4-fluorobenzyl)-*N*²-(2-methoxyethyl)-4-oxo-1,4-dihydropyridine-2,5-dicarboxamide (20). By use of compound 13, compound 20 was synthesized according to the method for synthesizing compound 14. ^1H NMR (CDCl_3) δ 3.27 (s, 3H), 3.76–3.40 (m, 2H), 3.47–3.52 (m, 2H), 4.63 (d, $J = 6.1$ Hz, 2H), 5.48 (s, 2H), 6.99–7.05 (m, 2H), 7.33–7.45 (m, 7H), 8.54–8.58 (m, 1H), 8.62 (d, $J = 6.7$ Hz, 1H), 10.44–10.48 (m, 1H).

1-Allyl-3-benzyloxy-*N*⁵-(4-fluorobenzyl)-*N*²-(2-methoxyethyl)-4-oxo-1,4-dihydropyridine-2,5-dicarboxamide (21). By use of compound 20, compound 21 was synthesized according to the method for synthesizing compound 15. ^1H NMR (CDCl_3) δ 3.21 (s, 3H), 3.32–3.35 (m, 2H), 3.38–3.45 (m, 2H), 4.58–4.61 (m, 4H), 5.14–5.30 (m, 4H), 5.82–5.93 (m, 1H), 6.72 (brs, 1H), 6.98–7.04 (m, 2H), 7.30–7.39 (m, 7H), 8.41 (s, 1H), 10.43–10.47 (m, 1H).

9-Benzyloxy-*N*-(4-fluorobenzyl)-3-hydroxy-2-(2-methoxyethyl)-1,8-dioxo-2,3,4,8-tetrahydro-1H-pyrido[1,2-*a*]pyrazine-7-carboxamide (22). By use of compound 21, compound 22 was synthesized according to the method for synthesizing compound 16. ^1H NMR (CDCl_3) δ 3.07–3.17 (m, 1H), 3.42 (s, 3H), 3.44–3.49 (m, 1H), 3.61–3.69 (m, 1H), 4.11–4.17 (m, 4H), 4.26–4.31 (m, 1H), 4.43–4.49 (m, 1H), 4.59–4.62 (m, 2H), 5.00–5.08 (m, 2H), 5.20 (d, $J = 9.9$ Hz, 1H), 5.34 (d, $J = 9.9$ Hz, 1H), 6.98–7.04 (m, 2H), 7.30–7.35 (m, 5H), 7.60–7.63 (m, 2H), 8.38 (s, 1H), 10.45–10.49 (m, 1H).

3,9-Dihydroxy-2-(2-methoxyethyl)-1,8-dioxo-1,3,4,8-tetrahydro-2H-pyrido[1,2-*a*]pyrazine-7-carboxylic Acid 4-Fluorobenzylamide (23). According to the method for synthesizing 19,

compound **23** was synthesized from **22**. Mp 163–164 °C; ¹H NMR (CDCl₃) δ 3.24–3.32 (m, 1H), 3.46 (s, 3H), 3.52–3.57 (m, 1H), 3.72–3.80 (m, 1H), 4.17–4.39 (m, 3H), 4.62 (d, *J* = 5.8 Hz, 2H), 5.12 (s, 1H), 5.80 (brs, 1H), 6.97–7.03 (m, 2H), 7.30–7.35 (m, 2H), 8.32 (s, 1H), 10.36–10.38 (m, 1H), 12.02 (brs, 1H). Anal. Calcd for C₁₉H₂₀FN₃O₆: C, 56.29; H, 4.97; F, 4.69; N, 10.37. Found: C, 56.13; H, 4.99; F, 4.55; N, 10.34.

7-Benzoyloxy-N-(4-fluorobenzyl)-6,8-dioxo-3,4,6,8,12,12a-hexahydro-2H-[1,3]oxazino[3,2-d]pyrido[1,2-a]pyrazine-9-carboxamide (25). To a solution of compound **16** (200 mg, 0.442 mmol) in dichloromethane (5 mL) were added 3-aminopropane-1-ol (35.0 μL, 0.511 mmol) and acetic acid (10.0 mg, 0.167 mmol). The reaction was performed with a microwave reaction apparatus at 140 °C for 30 min. After the mixture was cooled to room temperature, solvent was evaporated in vacuo, the residue was subjected to silica gel column chromatography, and fractions eluting with chloroform–methanol were collected and concentrated to obtain the product (173 mg, 74% yield) as a colorless solid. ¹H NMR (CDCl₃) δ 1.62–1.67 (m, 1H), 1.91–2.07 (m, 1H), 3.07 (dt, *J* = 12.9, 3.3 Hz, 1H), 3.84 (dt, *J* = 11.7, 2.4 Hz, 1H), 4.11–4.20 (m, 2H), 4.32 (dd, *J* = 13.8, 3.3 Hz, 1H), 4.63 (d, *J* = 6.0 Hz, 2H), 4.71–4.78 (m, 1H), 5.01 (t, *J* = 4.2 Hz, 1H), 5.26 (d, *J* = 9.9 Hz, 1H), 5.31 (d, *J* = 9.9 Hz, 1H), 7.00–7.07 (m, 2H), 7.32–7.42 (m, 5H), 7.64–7.66 (m, 2H), 8.39 (s, 1H), 10.45 (brs, 1H).

6-Benzoyloxy-N-(4-fluorobenzyl)-5,7-dioxo-2,3,5,7,11,11a-hexahydrooxazol[3,2-d]pyrido[1,2-a]pyrazine-8-carboxamide (24). ¹H NMR (DMSO-*d*₆) δ 3.52–3.62 (m, 1H), 3.78–3.91 (m, 1H), 4.01–4.12 (m, 2H), 4.24–4.31 (m, 1H), 4.50–4.62 (m, 2H), 4.88 (dd, *J* = 3.3, 12.0 Hz, 1H), 5.07 (d, *J* = 10.2 Hz, 1H), 5.21 (d, *J* = 10.2 Hz, 1H), 5.31 (dd, *J* = 9.9, 3.3 Hz, 1H), 7.19 (t, *J* = 8.7 Hz, 2H), 7.32–7.42 (m, 5H), 7.58 (d, *J* = 6.6 Hz, 2H), 8.64 (s, 1H), 10.49–10.54 (t, *J* = 6.3 Hz, 1H).

1-Benzoyloxy-2,11-dioxo-2,5,5a,7,8,9,10,11-octahydro-6-oxa-4a,10a-diazacyclohepta[b]naphthalene-3-carboxylic Acid 4-Fluorobenzylamide (26). ¹H NMR (CDCl₃) δ 1.55–1.60 (m, 1H), 1.77–1.91 (m, 2H), 2.03–2.13 (m, 1H), 3.13–3.22 (m, 1H), 3.64–3.81 (m, 2H), 4.15–4.21 (m, 1H), 4.31–4.37 (m, 1H), 4.39–4.48 (m, 1H), 4.63 (t, *J* = 6.0 Hz, 2H), 4.99 (t, *J* = 2.4 Hz, 1H), 5.26 (d, *J* = 10.2 Hz, 1H), 5.41 (d, *J* = 10.2 Hz, 1H), 7.03 (d, *J* = 9.0 Hz, 2H), 7.20–7.40 (m, 5H), 7.63–7.65 (m, 2H), 8.40 (s, 1H), 10.49–10.54 (m, 1H).

6-Benzoyloxy-N-(4-fluorobenzyl)-1-isopropyl-5,7-dioxo-2,3,5,7,11,11a-hexahydro-1H-imidazo[1,2-d]pyrido[1,2-a]pyrazine-8-carboxamide (27). ¹H NMR (DMSO-*d*₆) δ 1.06 (d, *J* = 6.3 Hz, 3H), 1.16 (d, *J* = 6.3 Hz, 3H), 2.77–2.85 (m, 1H), 2.98–3.07 (m, 1H), 3.15–3.22 (m, 1H), 3.54–3.58 (m, 2H), 3.87 (t, *J* = 11.4 Hz, 1H), 4.48–4.57 (m, 3H), 4.81–4.85 (m, 1H), 5.06 (d, *J* = 10.2 Hz, 1H), 5.20 (d, *J* = 10.2 Hz, 1H), 7.19 (t, *J* = 9.0 Hz, 2H), 7.31–7.42 (m, 5H), 7.57 (d, *J* = 7.8 Hz, 2H), 8.62 (s, 1H), 10.49 (t, *J* = 6.0 Hz, 1H).

5-Benzoyloxy-1-methyl-6,10-dioxo-1,2,3,4,6,9,9a,10-octahydro-1,4a,8a-triazaanthracene-7-carboxylic Acid 4-Fluorobenzylamide (28). ¹H NMR (CDCl₃) δ 1.61–1.68 (m, 2H), 2.31 (s, 3H), 2.85–2.93 (m, 1H), 3.06–3.11 (m, 1H), 4.32–4.39 (m, 2H), 4.58–4.66 (m, 3H), 4.69–4.79 (m, 2H), 5.32 (s, 2H), 7.02–7.08 (m, 2H), 7.33–7.42 (m, 5H), 7.64–7.66 (m, 2H), 8.41 (s, 1H), 10.50 (brs, 1H).

5-Benzoyloxy-1-isopropyl-6,10-dioxo-1,2,3,4,6,9,9a,10-octahydro-1,4a,8a-triazaanthracene-7-carboxylic Acid 4-Fluorobenzylamide (29). ¹H NMR (DMSO-*d*₆) δ 0.95–0.99 (m, 6H), 1.52–1.56 (m, 1H), 1.64–1.69 (m, 1H), 2.49–2.56 (m, 1H), 2.89–2.98 (m, 2H), 2.32–2.41 (m, 1H), 2.40–2.55 (m, 1H), 3.68–3.70 (m, 2H), 4.36 (brs, 1H), 4.54–4.59 (m, 1H), 4.88–4.93 (m, 1H), 5.07 (d, *J* = 10.2 Hz, 1H), 5.13 (d, *J* = 10.2 Hz, 1H), 7.18–7.24 (m, 2H), 7.35–7.45 (m, 5H), 7.58–7.62 (m, 2H), 8.78 (s, 1H), 10.52 (t, *J* = 6.0 Hz, 1H).

5-Benzoyloxy-6,10-dioxo-1-thiazol-2-ylmethyl-1,2,3,4,6,9,9a,10-octahydro-1,4a,8a-triazaanthracene-7-carboxylic Acid 4-Fluorobenzylamide (30). ¹H NMR (CDCl₃) δ 1.67–1.71 (m, 1H), 2.00–2.13 (m, 1H), 2.84–2.97 (m, 2H), 3.19–3.23 (m, 1H), 4.13 (s, 2H), 4.35–4.38 (m, 2H), 4.56–4.67 (m, 3H), 4.71–4.80 (m, 1H), 5.29 (d, *J* = 9.9 Hz, 1H), 5.36 (d, *J* = 9.9 Hz, 1H), 7.03–7.08 (m, 2H), 7.24 (d, *J* = 3.3 Hz, 1H), 7.34–7.42 (m, 5H),

7.66–7.69 (m, 2H), 7.79 (d, *J* = 3.3 Hz, 1H), 8.05 (brs, 1H), 10.49 (t, *J* = 6.0 Hz, 1H).

5-Benzoyloxy-1-(2-methoxyethyl)-6,10-dioxo-1,2,3,4,6,9,9a,10-octahydro-1,4a,8a-triazaanthracene-7-carboxylic Acid 4-Fluorobenzylamide (31). ¹H NMR (CDCl₃) δ 1.56–1.65 (m, 1H), 1.82–1.95 (m, 1H), 2.62–2.70 (m, 1H), 2.80–2.92 (m, 3H), 2.98–3.05 (m, 1H), 3.28–3.34 (m, 1H), 3.34 (s, 3H), 3.58–3.65 (m, 1H), 4.28 (dd, *J* = 13.8 Hz, 3.6 Hz, 1H), 4.38 (brs, 1H), 4.53–4.59 (m, 1H), 4.63 (d, *J* = 6.0 Hz, 2H), 4.69–4.76 (m, 1H), 5.29 (s, 2H), 7.00–7.05 (m, 2H), 7.30–7.38 (m, 5H), 7.63–7.66 (m, 2H), 8.38 (s, 1H), 10.53 (t, *J* = 6.0 Hz, 1H).

1-Benzoyloxy-6-methyl-2,11-dioxo-2,5a,6,7,8,9,10,11-octahydro-5H-4a,6,10a-triazacyclohepta[b]naphthalene-3-carboxylic Acid 4-Fluorobenzylamide (32). ¹H NMR (CDCl₃) δ 1.55–1.87 (m, 4H), 2.28 (s, 3H), 2.69–2.83 (m, 2H), 3.07–3.16 (m, 1H), 4.16–4.40 (m, 4H), 4.57–4.70 (m, 2H), 5.28 (d, *J* = 10.2 Hz, 1H), 5.39 (d, *J* = 10.2 Hz, 1H), 7.01–7.07 (m, 2H), 7.29–7.39 (m, 5H), 7.61–7.64 (m, 2H), 8.38 (s, 1H), 10.56 (t, *J* = 5.4 Hz, 1H).

1-Benzoyloxy-6-isobutyl-2,11-dioxo-2,5a,6,7,8,9,10,11-octahydro-5H-4a,6,10a-triazacyclohepta[b]naphthalene-3-carboxylic Acid 4-Fluorobenzylamide (33). ¹H NMR (CDCl₃) δ 0.87 (t, *J* = 6.6 Hz, 3H), 0.90 (d, *J* = 6.6 Hz, 3H), 1.57–1.71 (m, 4H), 1.79–1.86 (m, 1H), 2.31 (dd, *J* = 13.5, 7.5 Hz, 1H), 2.62 (dd, *J* = 13.5, 6.9 Hz, 1H), 2.75–2.95 (m, 2H), 3.02–3.09 (m, 1H), 4.06–4.21 (m, 2H), 4.33–4.40 (m, 1H), 4.48–4.51 (m, 1H), 4.56–4.70 (m, 2H), 5.28 (d, *J* = 9.9 Hz, 1H), 5.32 (d, *J* = 9.9 Hz, 1H), 7.04 (t, *J* = 8.7 Hz, 2H), 7.31–7.40 (m, 5H), 7.63 (d, *J* = 6.6 Hz, 2H), 8.36 (s, 1H), 10.54 (t, *J* = 6.0 Hz, 1H).

5-Benzoyloxy-6,10-dioxo-1,2,3,4,6,9,9a,10-octahydro-1,4a,8a-triazaanthracene-7-carboxylic Acid 4-Fluorobenzylamide (34). ¹H NMR (CDCl₃) δ 1.67–1.80 (m, 2H), 2.80–2.90 (m, 1H), 2.95–3.05 (m, 1H), 3.16–3.21 (m, 1H), 3.98 (dd, *J* = 13.2, 8.4 Hz, 1H), 4.23 (dd, *J* = 3.9 Hz, 1H), 4.55 (dd, *J* = 8.1, 3.9 Hz, 1H), 4.62 (d, *J* = 5.7 Hz, 2H), 4.65–4.68 (m, 1H), 5.23 (d, *J* = 10.2 Hz, 1H), 5.27 (d, *J* = 10.2 Hz, 1H), 7.00–7.06 (m, 2H), 7.33–7.41 (m, 5H), 7.63–7.66 (m, 2H), 8.37 (s, 1H), 10.47 (t, *J* = 5.7 Hz, 1H).

1-Acetyl-5-benzoyloxy-6,10-dioxo-1,2,3,4,6,9,9a,10-octahydro-1,4a,8a-triazaanthracene-7-carboxylic Acid 4-Fluorobenzylamide (35). To a solution of compound **34** (150 mg, 0.315 mmol) in pyridine (1.5 mL) were added acetic anhydride (60.0 μL, 0.630 mmol) and a catalytic amount of DMAP. After the mixture was stirred for 5 h at room temperature, 2 M aqueous HCl (20 mL) was added to the mixture and extracted with ethyl acetate. The combined organics were washed with water and dried over anhydrous sodium sulfate and concentrated in vacuo. The residue was recrystallized with chloroform to give the product (126 mg, 77% yield) as an orange solid. ¹H NMR (DMSO-*d*₆) δ 1.85–2.18 (m, 2H), 2.18 (s, 3H), 2.45–2.54 (m, 1H), 2.83–2.94 (m, 1H), 3.28–3.36 (m, 1H), 4.40–4.57 (m, 5H), 5.07 (d, *J* = 10.2 Hz, 1H), 5.15 (d, *J* = 10.2 Hz, 1H), 6.10 (brs, 1H), 7.19 (t, *J* = 8.7 Hz, 2H), 7.34–7.43 (m, 5H), 7.59 (d, *J* = 6.9 Hz, 2H), 8.64 (s, 1H), 10.49 (d, *J* = 5.7 Hz, 1H).

5-Benzoyloxy-1-methanesulfonyl-6,10-dioxo-1,2,3,4,6,9,9a,10-octahydro-1,4a,8a-triazaanthracene-7-carboxylic Acid 4-Fluorobenzylamide (36). To a solution of compound **34** (150 mg, 0.315 mmol) in pyridine (1.5 mL) were added methanesulfonyl chloride (37.0 μL, 0.473 mmol) and a catalytic amount of DMAP. After the mixture was stirred for 3.5 h at room temperature, 2 M aqueous HCl was added to the mixture and extracted with ethyl acetate. The combined organics were washed with water and dried over anhydrous sodium sulfate and concentrated in vacuo. The residue was recrystallized with chloroform–diisopropyl ether to give the product (86.0 mg, 49% yield) as colorless crystals. ¹H NMR (DMSO-*d*₆) δ 1.78–1.87 (m, 1H), 1.95–2.02 (m, 1H), 2.98–3.08 (m, 1H), 3.20 (s, 3H), 3.40–3.53 (m, 1H), 3.58–3.67 (m, 1H), 4.48–4.64 (m, 4H), 4.74–4.85 (m, 1H), 5.08–5.17 (m, 2H), 5.59–5.63 (m, 1H), 7.21 (t, *J* = 9.0 Hz, 2H), 7.36–7.44 (m, 5H), 7.59–7.66 (m, 2H), 8.58 (s, 1H), 10.47 (t, *J* = 6.3 Hz, 1H).

5-Hydroxy-4,6-dioxo-2,3,4,6,9,9a-hexahydro-1-oxa-3a,8a-diazacyclopenta[b]naphthalene-7-carboxylic Acid 4-Fluorobenzylamide (37). Mp 272–274 °C; ¹H NMR (DMSO-*d*₆) δ 3.59–3.67 (m, 1H), 3.72–3.81 (m, 1H), 3.98–4.10 (m, 2H), 4.27–

4.35 (m, 1H), 4.52 (d, $J = 7.2$ Hz, 2H), 4.92 (dd, $J = 12.3, 12.3$ Hz, 1H), 5.27 (dd, $J = 9.9, 3.6$ Hz, 1H), 7.11–7.20 (m, 2H), 7.30–7.40 (m, 2H), 8.49 (s, 1H), 10.32 (t, $J = 5.6$ Hz, 1H), 11.53 (s, 1H). Anal. Calcd for $C_{18}H_{16}FN_3O_5$: C, 57.91; H, 4.32; F, 5.09; N, 11.26. Found: C, 57.78; H, 4.28; F, 4.97; N, 11.25.

5-Hydroxy-6,10-dioxo-3,4,6,9,9a,10-hexahydro-2H-1-oxa-4a,8a-diazaanthracene-7-carboxylic Acid 4-Fluorobenzylamide (38). Mp 259–259 °C; 1H NMR (DMSO- d_6) δ 1.60–1.67 (m, 1H), 1.72–1.85 (m, 1H), 3.25 (td, $J = 12.8, 3.5$ Hz, 1H), 3.86–3.93 (m, 1H), 4.06 (dd, $J = 11.4, 4.2$ Hz, 1H), 4.44–4.57 (m, 5H), 5.28 (t, $J = 3.8$ Hz, 1H), 7.13–7.18 (m, 2H), 7.33–7.37 (m, 2H), 8.51 (s, 1H), 10.36 (t, $J = 6.0$ Hz, 1H), 12.47 (s, 1H). Anal. Calcd for $C_{19}H_{18}FN_3O_5$: C, 58.91; H, 4.68; F, 4.90; N, 10.85. Found: C, 58.86; H, 4.65; F, 4.74; N, 10.85.

1-Hydroxy-2,11-dioxo-2,5,5a,7,8,9,10,11-octahydro-6-oxa-4a,10a-diazacyclohepta[b]naphthalene-3-carboxylic Acid 4-Fluorobenzylamide (39). Mp 242–244 °C; 1H NMR (DMSO- d_6) δ 1.40–2.00 (m, 4H), 3.20–3.30 (m, 1H), 3.66–3.77 (m, 2H), 4.14–4.23 (m, 1H), 4.38–4.41 (m, 1H), 4.52 (d, $J = 6.3$ Hz, 2H), 4.58–4.63 (m, 1H), 5.34 (brs, 1H), 7.15 (t, $J = 9.0$ Hz, 2H), 7.33–7.37 (m, 2H), 8.50 (s, 1H), 10.39 (brs, 1H), 12.14 (s, 1H). Anal. Calcd for $C_{20}H_{20}FN_3O_5(H_2O)_{0.3}$: C, 59.05; H, 5.10; F, 4.67; N, 10.33. Found: C, 59.15; H, 4.95; F, 4.52; N, 10.30.

5-Hydroxy-1-isopropyl-4,6-dioxo-2,3,4,6,9,9a-hexahydro-1H-1,3a,8a-triazacyclohepta[b]naphthalene-7-carboxylic Acid 4-Fluorobenzylamide (40). Mp 232–234 °C; 1H NMR (DMSO- d_6) δ 1.03 (d, $J = 6.6$ Hz, 3H), 1.14 (d, $J = 6.6$ Hz, 3H), 2.70–2.90 (m, 1H), 2.90–3.10 (m, 1H), 3.12–3.30 (m, 1H), 3.40–3.66 (m, 2H), 3.82 (t, $J = 10.8$ Hz, 1H), 4.40–4.60 (m, 3H), 4.90 (d, $J = 12.3$ Hz, 1H), 7.10–7.20 (m, 2H), 7.30–7.40 (m, 2H), 8.45 (s, 1H), 10.39 (t, $J = 5.4$ Hz, 1H), 11.60 (s, 1H). Anal. Calcd for $C_{21}H_{23}FN_4O_4$: C, 60.86; H, 5.59; F, 4.58; N, 13.52. Found: C, 60.61; H, 5.51; F, 4.47; N, 13.43.

5-Hydroxy-1-methyl-6,10-dioxo-1,2,3,4,6,9,9a,10-octahydro-1,4a,8a-triazaanthracene-7-carboxylic Acid 4-Fluorobenzylamide (41). Mp 252–253 °C; 1H NMR (DMSO- d_6) δ 1.56–1.75 (m, 2H), 2.22 (s, 3H), 2.50–2.55 (m, 1H), 2.90–3.10 (m, 2H), 4.17 (brs, 1H), 4.39–4.42 (m, 2H), 4.52 (d, $J = 6.0$ Hz, 2H), 4.74–4.78 (m, 1H), 7.13–7.17 (m, 2H), 7.33–7.37 (m, 2H), 8.61 (s, 1H), 10.40 (t, $J = 6.0$ Hz, 1H), 12.54 (s, 1H). Anal. Calcd for $C_{20}H_{21}FN_4O_4$: C, 59.99; H, 5.29; F, 4.74; N, 13.99. Found: C, 59.61; H, 5.30; F, 4.55; N, 13.81.

5-Hydroxy-1-isopropyl-6,10-dioxo-1,2,3,4,6,9,9a,10-octahydro-1,4a,8a-triazaanthracene-7-carboxylic Acid 4-Fluorobenzylamide (42). Mp 220 °C; 1H NMR (DMSO- d_6) δ 0.94 (d, $J = 9.6$ Hz, 6H), 1.53–1.67 (m, 2H), 2.92–3.30 (m, 3H), 4.32–4.40 (m, 4H), 4.52 (d, $J = 5.7$ Hz, 2H), 4.89 (d, $J = 14.1$ Hz, 1H), 7.16 (t, $J = 9.0$ Hz, 2H), 7.35 (dd, $J = 9.0, 6.3$ Hz, 2H), 8.61 (s, 1H), 10.46 (s, 1H), 12.55 (s, 1H). Anal. Calcd for $C_{22}H_{23}FN_4O_4(H_2O)_{1.0}$: C, 59.18; H, 6.10; F, 4.26; N, 12.55. Found: C, 59.13; H, 5.76; F, 4.07; N, 12.41.

5-Hydroxy-6,10-dioxo-1-(thiazol-2-yl)methyl-1,2,3,4,6,9,9a,10-octahydro-1,4a,8a-triazaanthracene-7-carboxylic Acid 4-Fluorobenzylamide (43). Mp 214–215 °C; 1H NMR (DMSO- d_6) δ 1.54–1.72 (m, 2H), 2.75–2.81 (m, 1H), 2.95–3.07 (m, 2H), 3.80 (d, $J = 16.0$ Hz, 1H), 4.37 (d, $J = 16.4$ Hz, 1H), 4.44–4.51 (m, 4H), 4.69 (brs, 1H), 4.89–4.93 (m, 1H), 7.13–7.17 (m, 2H), 7.32–7.35 (m, 2H), 7.55 (d, $J = 3.2$ Hz, 1H), 7.69 (d, $J = 3.2$ Hz, 1H), 8.37 (s, 1H), 10.36 (t, $J = 6.0$ Hz, 1H), 12.50 (s, 1H). Anal. Calcd for $C_{23}H_{22}FN_5O_4S(H_2O)_{0.4}$: C, 56.29; H, 4.68; F, 3.87; N, 14.27; S, 6.53. Found: C, 56.49; H, 4.59; F, 3.78; N, 14.12; S, 6.25.

5-Hydroxy-1-(2-methoxyethyl)-6,10-dioxo-1,2,3,4,6,9,9a,10-octahydro-1,4a,8a-triazaanthracene-7-carboxylic Acid 4-Fluorobenzylamide (44). Mp 147 °C; 1H NMR (DMSO- d_6) δ 1.56–1.74 (m, 2H), 2.53–2.58 (m, 1H), 2.66–3.10 (m, 4H), 3.18 (s, 3H), 3.41–3.39 (m, 2H), 4.37–4.52 (m, 5H), 4.73–4.80 (m, 1H), 7.15 (t, $J = 8.8$ Hz, 2H), 7.33–7.37 (m, 2H), 8.56 (s, 1H), 10.40 (t, $J = 6.0$ Hz, 1H), 12.62 (s, 1H). LC/MS: m/z 445 $[M + H]^+$.

1-Hydroxy-6-methyl-2,11-dioxo-2,5a,6,7,8,9,10,11-octahydro-5H-4a,6,10a-triazacyclohepta[b]naphthalene-3-carboxylic Acid 4-Fluorobenzylamide (45). Mp 230–231 °C; 1H NMR (DMSO- d_6) δ 1.47–1.53 (m, 1H), 1.62–1.78 (m, 3H), 2.29 (s, 3H), 2.77–2.81 (m, 2H), 4.05–4.10 (m, 1H), 4.35–4.40 (m, 1H), 4.54–4.64 (m, 3H), 4.70 (s, 1H), 7.18–7.22 (m, 2H), 7.30–7.34 (m, 1H),

7.47–7.52 (m, 1H), 8.49 (s, 1H), 10.47 (d, $J = 6.0$ Hz, 1H), 12.44 (s, 1H). Anal. Calcd for $C_{21}H_{23}FN_4O_4$: C, 60.86; H, 5.59; F, 4.58; N, 13.52. Found: C, 60.46; H, 5.57; F, 4.52; N, 13.23.

1-Hydroxy-6-isobutyl-2,11-dioxo-2,5a,6,7,8,9,10,11-octahydro-5H-4a,6,10a-triazacyclohepta[b]naphthalene-3-carboxylic Acid 4-Fluorobenzylamide (46). Mp 221–223 °C; 1H NMR (DMSO- d_6) δ 0.81 (d, $J = 6.8$ Hz, 3H), 0.84 (d, $J = 6.4$ Hz, 3H), 1.45–1.78 (m, 5H), 2.36–2.54 (m, 2H), 2.27–2.93 (m, 2H), 3.17–3.23 (m, 1H), 4.03–4.06 (m, 1H), 4.32–4.56 (m, 4H), 4.82–4.85 (m, 1H), 7.13–7.17 (m, 2H), 7.30–7.37 (m, 2H), 8.48 (s, 1H), 10.42 (t, $J = 6.0$ Hz, 1H), 12.53 (s, 1H). Anal. Calcd for $C_{24}H_{29}FN_4O_4(H_2O)_{0.3}$: C, 62.40; H, 6.46; F, 4.11; N, 12.13. Found: C, 62.50; H, 6.34; F, 4.22; N, 11.97.

1-Acetyl-5-hydroxy-6,10-dioxo-1,2,3,4,6,9,9a,10-octahydro-1,4a,8a-triazaanthracene-7-carboxylic Acid 4-Fluorobenzylamide (47). Mp 290 °C; 1H NMR (DMSO- d_6) δ 1.78–2.14 (m, 2H), 2.14 (s, 3H), 2.80–3.00 (m, 2H), 4.05–4.15 (m, 1H), 4.30–4.60 (m, 3H), 4.51 (d, $J = 5.7$ Hz, 2H), 5.99 (s, 1H), 7.15 (t, $J = 9.0$ Hz, 2H), 7.30–7.40 (m, 2H), 8.37 (s, 1H), 10.46 (s, 1H), 12.28 (s, 1H). Anal. Calcd for $C_{21}H_{21}FN_4O_5(H_2O)_{0.5}$: C, 57.66; H, 5.07; F, 4.34; N, 12.81. Found: C, 57.53; H, 4.90; F, 4.20; N, 12.64.

5-Hydroxy-1-methanesulfonyl-6,10-dioxo-1,2,3,4,6,9,9a,10-octahydro-1,4a,8a-triazaanthracene-7-carboxylic Acid 4-Fluorobenzylamide (48). Mp 257–259 °C; 1H NMR (DMSO- d_6) δ 1.80–1.96 (m, 2H), 3.02–3.58 (m, 2H), 3.16 (s, 3H), 4.52 (d, $J = 5.7$ Hz, 2H), 4.50–4.60 (m, 1H), 4.70–4.80 (m, 1H), 5.56 (s, 1H), 7.16 (t, $J = 9.0$ Hz, 2H), 8.36 (s, 1H), 10.39 (s, 1H). LC/MS: m/z 465 $[M + H]^+$.

6.2. Biological Assay and PK Studies in Rats. All biological and PK studies were performed in the same manner as described in our previous paper.¹¹

AUTHOR INFORMATION

Corresponding Author

*Telephone: +81-6-6331-6349. Fax: +81-6-6332-6385. E-mail: takashi.kawasuji@shionogi.co.jp.

Notes

The authors declare no competing financial interest.

ACKNOWLEDGMENTS

The authors thank all scientists on the Shionogi–GlaxoSmithKline research collaboration team for great discussions, in particular Shuji Iwashita and Eri Kanaoka for PK evaluations and Akemi Kagitani-Suyama, Shigeru Miki, and Shinobu Miki-Kawauchi for antiviral evaluations.

ABBREVIATIONS USED

CYP3A, cytochrome P450, family 3, subfamily A; HOBt, 1-hydroxybenzotriazole; rt, room temperature; NaOMe, sodium methoxide; MnO₂, manganese dioxide; TFA, trifluoroacetic acid; BnBr, benzyl bromide; CO, carbon monoxide; 10% Pd–C, palladium carbon; Pd(OAc)₂, palladium diacetate; Ac₂O, acetic anhydride; MsCl, methanesulfonyl chloride; NaOH, sodium hydroxide; DMAP, *N,N*-dimethylaminopyridine; Et₃N, triethylamine; NH₃, ammonia; CDCl₃, deuterated chloroform; DMSO- d_6 , deuterated DMSO; HCl, hydrogen chloride; Na₂CO₃, sodium carbonate; Cs₂CO₃, cesium carbonate; K₂CO₃, potassium carbonate; Na₂SO₄, sodium sulfate; Et₂O, diethyl ether; NaHSO₃, sodium hydrogen sulfite

REFERENCES

- (1) (a) Hazuda, D. J. HIV Integrase as a Target for Antiretroviral Therapy. *Curr. Opin. HIV AIDS* 2012, 7, 383–389. (b) Adams, J. L.; Greener, B. N.; Kashuba, A. D. M. Pharmacology of HIV Integrase Inhibitors. *Curr. Opin. HIV AIDS* 2012, 7, 390–400. (c) Pendri, A.; Meanwell, N. A.; Peese, K. M.; Walker, M. A. New First and Second

Generation Inhibitors of Human Immunodeficiency Virus-1 Integrase. *Expert Opin. Ther. Pat.* **2011**, *21*, 1173–1189. (d) Johns, B. A.; Svolto, A. C. Advances in Two-Metal Chelation Inhibitors of HIV Integrase. *Expert Opin. Ther. Pat.* **2008**, *18*, 1225–1237. (e) Grobler, J. A.; Stillmock, K.; Hu, B.; Witmer, M.; Felock, P.; Espeseth, A. S.; Wolfe, A.; Egbertson, M.; Bourgeois, M.; Melamed, J.; Wai, J. S.; Young, S.; Vacca, J.; Hazuda, D. J. Diketo Acid Inhibitor Mechanism and HIV-1 Integrase: Implications for Metal Binding in the Active Site of Phosphotransferase Enzymes. *Proc. Natl. Acad. Sci. U.S.A.* **2002**, *99*, 6661–6666. (f) Hazuda, D. J.; Felock, P.; Witmer, M.; Wolfe, A.; Stillmock, K.; Grobler, J. A.; Espeseth, A.; Gabryelski, L.; Schleif, W.; Blau, C.; Miller, M. D. Inhibitors of Strand Transfer That Prevent Integration and Inhibit HIV-1 Replication in Cells. *Science* **2000**, *28*, 646–650.

(2) (a) Rowley, M. The Discovery of Raltegravir, an Integrase Inhibitor for the Treatment of HIV Infection. *Prog. Med. Chem.* **2008**, *46*, 1–28. (b) Summa, V.; Petrocchi, A.; Bonelli, F.; Crescenzi, B.; Donghi, M.; Ferrara, M.; Fiore, F.; Gardelli, C.; Gonzalez Paz, O.; Hazuda, D. J.; Jones, P.; Kinzel, O.; Laufer, R.; Monteagudo, E.; Muraglia, E.; Nizi, E.; Orvieto, F.; Pace, P.; Pescatore, G.; Scarpelli, R.; Stillmock, K.; Witmer, M. V.; Rowley, M. Discovery of Raltegravir, a Potent, Selective Orally Bioavailable HIV-Integrase Inhibitor for the Treatment of HIV-AIDS Infection. *J. Med. Chem.* **2008**, *51*, 5843–5855.

(3) (a) Thompson, M. A.; Aberg, J. A.; Cahn, P.; Montaner, J. S.; Rizzardini, G.; Telenti, A.; Gatell, J. M.; Günthard, H. F.; Hammer, S. M.; Hirsch, M. S.; Jacobsen, D. M.; Reiss, P.; Richman, D. D.; Volberding, P. A.; Yeni, P.; Schooley, R. T. Antiretroviral Treatment of Adult HIV Infection: 2010 Recommendations of the International AIDS Society-USA Panel. *JAMA, J. Am. Med. Assoc.* **2010**, *304*, 321–333. (b) Thompson, M. A.; Aberg, J. A.; Hoy, J. F.; Telenti, A.; Benson, C.; Cahn, P.; Eron, J. J.; Günthard, H. F.; Hammer, S. M.; Reiss, P.; Richman, D. D.; Rizzardini, G.; Thomas, D. L.; Jacobsen, D. M.; Volberding, P. A. Antiretroviral Treatment of Adult HIV Infection: 2012 Recommendations of the International Antiviral Society-USA Panel. *JAMA, J. Am. Med. Assoc.* **2012**, *308*, 387–402. Guidelines for the Use of Antiretroviral Agents in HIV-1-Infected Adults and Adolescents: DHHS Panel. December 1, 2009.

(4) (a) Cooper, D. A.; Steigbigel, R. T.; Gatell, J. M.; Rockstroh, J. K.; Katlama, C.; Yeni, P.; Lazzarin, A.; Clotet, B.; Kumar, P. N.; Eron, J. E.; Schechter, M.; Markowitz, M.; Loutfy, M. R.; Lennox, J. L.; Zhao, J.; Chen, J.; Ryan, D. M.; Rhodes, R. R.; Killar, J. A.; Gilde, L. R.; Strohmaier, K. L.; Meibohm, A. R.; Miller, M. D.; Hazuda, D. J.; Nessler, M. L.; DiNubile, M. J.; Isaacs, R. D.; Tepller, H.; Nguyen, B. Y.; BENCHMRK Study Teams. Subgroup and Resistance Analyses of Raltegravir for Resistant HIV-1 Infection. *N. Engl. J. Med.* **2008**, *359*, 355–365. (b) Marcelin, A. G.; Ceccherini Silberstein, F.; Perno, C. F.; Calvez, V. Resistance to Novel Drug Classes. *Curr. Opin. HIV AIDS* **2009**, *4*, 531–537.

(5) (a) Shimura, K.; Kodama, E.; Sakagami, Y.; Matsuzaki, Y.; Watanabe, W.; Yamataka, K.; Watanabe, Y.; Ohata, Y.; Doi, S.; Sato, M.; Kano, M.; Ikeda, S.; Matsuoka, M. Broad Antiretroviral Activity and Resistance Profile of the Novel Human Immunodeficiency Virus Integrase Inhibitor Elvitegravir (JTK-303/GS-9137). *J. Virol.* **2008**, *82*, 764–774. (b) Sato, M.; Kawakami, H.; Motomura, T.; Aramaki, H.; Matsuda, T.; Yamashita, M.; Ito, Y.; Matsuzaki, Y.; Yamataka, K.; Ikeda, S.; Shinkai, H. Quinolone Carboxylic Acids as a Novel Monoketo Acid Class of Human Immunodeficiency Virus Type 1 Integrase Inhibitors. *J. Med. Chem.* **2009**, *52*, 4869–4882.

(6) (a) Molina, J. M.; LaMarca, A.; Andrade-Villanueva, J.; Clotet, B.; Clumeck, N.; Liu, Y. P.; Zhong, L.; Margot, N.; Cheng, A. K.; Chuck, S. L.; Study 145 Team. Efficacy and Safety of Once Daily Elvitegravir versus Twice Daily Raltegravir in Treatment-Experienced Patients with HIV-1 Receiving a Ritonavir-Boosted Protease Inhibitor: Randomised, Double-Blind, Phase 3, Non-Inferiority Study. *Lancet Infect. Dis.* **2012**, *12*, 27–35. (b) Elion, R.; Gathe, J.; Rashbaum, B.; Shalit, P.; Hawkins, T.; Liu, H.; Zhong, L.; Warren, D.; Kearney, B.; Chuck, S. The Single-Tablet Regimen Elvitegravir/Cobicistat/Emtricitabine/Tenofovir Disoproxil Fumarate (EVG/COBI/FTC/TDF; “QUAD”) Maintains a

High Rate of Virologic Suppression, and Cobicistat (COBI) Is an Effective Pharmacoenhancer through 48 Weeks. Presented at the 50th Interscience Conference on Antimicrobial Agents and Chemotherapy, Boston, MA, September 12–15, 2010. (c) Cohen, C.; Shambraw, D.; Ruane, P.; Elion, R.; DeJesus, E.; Liu, H.; Zhong, L.; Warren, D.; Kearney, B.; Chuck, S. Single-Tablet, Fixed-Dose Regimen of Elvitegravir/Emtricitabine/Tenofovir Disoproxil Fumarate/GS-9350 Achieves a High Rate of Virologic Suppression and GS-9350 Is an Effective Booster. Presented at the 17th Conference on Retroviruses and Opportunistic Infections, San Francisco, CA, February 16–19, 2010.

(7) (a) Goethals, O.; Clayton, R.; Van Ginderen, M.; Vereyken, I.; Wagemans, E.; Geluykens, P.; Dockx, K.; Strijbos, R.; Smits, V.; Vos, A.; Meersseman, G.; Jochmans, D.; Vermeire, K.; Schols, D.; Hallenberger, S.; Hertogs, K. Resistance Mutations in Human Immunodeficiency Virus Type 1 Integrase Selected with Elvitegravir Confer Reduced Susceptibility to a Wide Range of Integrase Inhibitors. *J. Virol.* **2008**, *82*, 10366–10374. (b) Shimura, K.; Kodama, E.; Sakagami, Y.; Matsuzaki, Y.; Watanabe, W.; Yamataka, K.; Watanabe, Y.; Ohata, Y.; Doi, S.; Sato, M.; Kano, M.; Ikeda, S.; Matsuoka, M. Broad Antiretroviral Activity and Resistance Profile of the Novel Human Immunodeficiency Virus Integrase Inhibitor Elvitegravir (JTK-303/GS-9137). *J. Virol.* **2008**, *82*, 764–774. (c) Marinello, J.; Marchand, C.; Mott, B. T.; Bain, A.; Thomas, C. J.; Pommier, Y. Comparison of Raltegravir and Elvitegravir on HIV-1 Integrase Catalytic Reactions and on a Series of Drug-Resistant Integrase Mutants. *Biochemistry* **2008**, *47*, 9345–9354. (d) Garrido, C.; Villacianb, J.; Zahoneroa, N.; Patteryb, T.; Garcaci, F.; Gutierrezd, F.; Caballeroe, E.; Houtteb, M. V.; Sorianoa, V.; Mendozaa, C.; SINRES Group. Broad Phenotypic Cross-Resistance to Elvitegravir in HIV-Infected Patients Failing on Raltegravir-Containing Regimens. *Antimicrob. Agents Chemother.* **2012**, *56*, 2873–2878. (e) Blanco, J.; Varghese, V.; Rhee, S.; Gtell, J.; Shafer, R. HIV-1 Integrase Inhibitor Resistance and Its Clinical Implications. *J. Infect. Dis.* **2011**, *203*, 1204–1214.

(8) Nachea, J. B.; Parienti, J.; Uthman, O.; Dowdy, D. W.; Mills, E. J.; Marco, V.; Giordano, T. P. Regimen Simplification in HIV Infection toward Once-Daily Dosing and Fixed-Dose Combinations: A Meta-Analysis and Sequential Analysis of Randomized Controlled Trials. TUPE096. Presented at the XIX International AIDS Conference, Washington, DC, July 22–27, 2012.

(9) (a) Kobayashi, M.; Yoshinaga, T.; Seki, T.; Wakasa-Morimoto, C.; Brown, K. W.; Ferris, R.; Foster, S. A.; Hazen, R. J.; Miki, S.; Suyama-Kagitani, A.; Kawachi-Miki, S.; Taishi, T.; Kawasuji, T.; Johns, A. B.; Underwood, R. M.; Garvey, P. E.; Sato, A.; Fujiwara, T. In Vitro Antiretroviral Properties of S/GSK1349572, a Next-Generation HIV Integrase Inhibitor. *Antimicrob. Agents Chemother.* **2011**, *55*, 813–821. (b) Hightower, K. E.; Wang, R.; DeAnda, F.; Johns, B. A.; Weaver, K.; Shen, Y.; Tomberlin, G. H.; Carter, H. L., III; Broderick, T.; Sigethy, S.; Seki, T.; Kobayashi, M.; Underwood, M. R. Dolutegravir (S/GSK1349572) Exhibits Significantly Slower Dissociation than Raltegravir and Elvitegravir from Wild-Type and Integrase Inhibitor-Resistant HIV-1 Integrase-DNA Complexes. *Antimicrob. Agents Chemother.* **2011**, *55*, 4552–4559.

(10) (a) Hazuda, D. J.; Young, S. D. Inhibitors of Human Immunodeficiency Virus Integration. *Adv. Antiviral Drug Des.* **2003**, *4*, 63–77. (b) Long, Y.; Jiang, X.; Dayam, R.; Sanchez, T.; Shoemaker, R.; Sei, S.; Neamati, N. Rational Design and Synthesis of Novel Dimeric Diketoacid-Containing Inhibitors of HIV-1 Integrase: Implication for Binding to Two Metal Ions on the Active Site of Integrase. *J. Med. Chem.* **2004**, *47*, 2561–2573. (c) Kawasuji, T.; Fuji, M.; Yoshinaga, T.; Sato, A.; Fujiwara, T.; Kiyama, R. A Platform for Designing HIV Integrase Inhibitors. Part 2: A Two-Metal Binding Model as a Potential Mechanism of HIV Integrase Inhibitors. *Bioorg. Med. Chem.* **2006**, *14*, 8420–8429. (d) Bacchi, A.; Carcelli, M.; Compari, C.; Fiscaro, E.; Pala, N.; Rispoli, G.; Rogolino, D.; Sanchez, T. W.; Sechi, M.; Neamati, N. HIV-1 IN Strand Transfer Chelating Inhibitors: A Focus on Metal Binding. *Mol. Pharmaceutics* **2011**, *8*, 507–519. (e) Bacchi, A.; Carcelli, M.; Compari, C.; Fiscaro, E.; Pala,

N.; Rispoli, G.; Rogolino, D.; Sanchez, T. W.; Sechi, M.; Sinisi, V.; Neamati, N. Investigating the Role of Metal Chelation in HIV-1 Integrase Strand Transfer Inhibitors. *J. Med. Chem.* **2011**, *54*, 8407–8420.

(11) Kawasuji, T.; Johns, B. A.; Yoshida, H.; Taishi, T.; Taoda, Y.; Murai, H.; Kiyama, R.; Fuji, M.; Yoshinaga, T.; Seki, T.; Kobayashi, M.; Sato, A.; Fujiwara, T. Carbamoyl Pyridone HIV-1 Integrase Inhibitors. I. Molecular Design and Establishment of an Advanced Two-Metal Binding Pharmacophore. *J. Med. Chem.* **2012**, *55*, 8735–8744.